Case Studies in Construction Materials 24 (2026) e05769

Contents lists available at ScienceDirect

Case Studies in Construction Materials

journal homepage: www.elsevier.com/locate/cscm

Case study

Effect of Sugarcane Bagasse Ash on the sustainable performance of hot-mix asphalt: A case study of experimental and numerical analysis

Udeme Udo Imoh [a], Adeyemi Oluwaseun Adeboje [b], Ebunlomo Ruth Adekola [b], Rauf Hassan [c], Majid Movahedi Rad [a,*]

[a] Department of Structural and Geotechnical Engineering, Faculty of Architecture, Civil Engineering and Transport Sciences, Széchenyi István University, Győr H-9026, Hungary
[b] Department of Civil Engineering, University of Lagos, Lagos 101017, Nigeria
[c] Department of Materials, Mechanics, Management & Design (3MD), Faculty of Civil Engineering & Geosciences, Delft University of Technology, Stevinweg 1, Delft 2628 CN, Netherlands

ARTICLE INFO

Keywords:
Hot mix asphalt (HMA)
Sugarcane Bagasse Ash (SBA)
Sustainable pavement
Marshall stability
Indirect tensile strength
Finite element modelling

ABSTRACT

The growing demand for sustainable road infrastructure has intensified the interest in alternative mineral fillers that reduce natural resource consumption and environmental impacts. This study investigates the use of Sugarcane Bagasse Ash (SBA), an abundant agricultural by-product in sub-Saharan Africa, as a partial replacement for conventional mineral fillers in hot-mix asphalt (HMA). Unlike previous studies that considered SBA primarily as a minor additive, this study provides a systematic evaluation across a wide replacement range (0–16 %), combined with experimental testing and numerical validation. Marshall and indirect tensile strength (ITS) tests were conducted on HMA mixtures produced using locally sourced Nigerian aggregates and 60/70 penetration-grade bitumen. A three-dimensional finite element model (FEM) of the ITS configuration was developed to corroborate the experimental response and identify stress concentration zones. results indicate that SBA improves both mechanical and volumetric performance within an optimal replacement range of 6–10 %, with peak performance of approximately 8 % SBA. Within this range, Marshall stability increased from 7.6 kN to 9.0 kN, the Marshall quotient reached 3.3 kN/mm, bulk density increased to 2.51 g/cm^3, and air voids decreased from 4.9 % to 3.5 %, remaining within standard design limits. Microstructural analyses confirmed the predominance of amorphous silica and porous SBA morphology, which promoted enhanced filler–binder interactions and mixture densification. FEM predictions of peak tensile stress agreed with laboratory ITS results within 10 % and successfully reproduced observed crack initiation zones. Excessive SBA content (> 10 %) led to reduced stability and density owing to over-filling effects. The findings demonstrate that 6–10 % SBA is a technically viable and sustainable filler replacement for HMA, particularly in sugarcane-producing regions, offering improved performance alongside waste valorization and reduced reliance on quarry-derived fillers.

* Corresponding author.
E-mail address: majidmr@sze.hu (M. Movahedi Rad).

https://doi.org/10.1016/j.cscm.2026.e05769
Received 23 August 2025; Received in revised form 28 December 2025; Accepted 5 January 2026
Available online 6 January 2026

1. Introduction

The rapid expansion of global transportation networks coupled with the pressing need for environmental conservation has spurred growing interest in the development of sustainable and cost-effective materials for road construction [1–5]. Hot-mix asphalt (HMA), the predominant material used in flexible pavement construction, is traditionally composed of coarse and fine aggregates, filler materials, and bituminous binders [6–8]. While HMA offers advantages such as cost efficiency, flexibility, and recyclability, its reliance on non-renewable natural resources and energy-intensive materials such as limestone filler and Portland cement poses significant environmental challenges. In addition, the production of bitumen and conventional asphalt mixtures results in high energy consumption and substantial greenhouse gas emissions, particularly carbon dioxide (CO_2), further exacerbating concerns regarding climate change and resource depletion [9–12]. To address these challenges, researchers and engineers are increasingly exploring the incorporation of industrial and agricultural by-products into asphalt mixtures, not only as a means to improve performance but also to promote waste recycling and environmental sustainability [10,11,13].

Recent studies have investigated the use of various waste materials to modify asphalt binders and mixtures. For instance, cathode-ray-tube (CRT) glass powder has been used as a filler replacement to improve the mechanical and aging resistance properties of asphalt composites, highlighting the potential of glass waste valorization in pavement materials [14–16]. Composite systems derived from stamp sand and acrylonitrile styrene acrylate (ASA) waste have shown promising results as alternative road-surfacing materials, demonstrating satisfactory stability and deformation resistance even in the absence of bitumen [17–21]. Rubber-based waste materials are at the forefront of sustainable pavement research. Rubber-modified asphalt mixtures incorporating tire-derived aggregates exhibit improved load-bearing capacity and reduced permanent deformation under high-stress conditions, suggesting enhanced resilience for subgrade applications [22–25]. Similarly, field demonstrations of asphalt overlays with recycled rubber and tire fabric fibers have shown significant improvements in fatigue life and cracking resistance, validating the laboratory findings at a practical implementation scale [26]. Moreover, the use of stress-absorbing membrane interlayers in resurfacing rubber-modified asphalt mixtures has proven effective in delaying reflective cracking and extending the pavement service life [27].

These contemporary studies underscore the growing consensus that incorporating waste-derived materials into asphalt systems can significantly enhance mechanical performance, extend service life, and align with circular economic goals [28]. Within this broad framework, Sugarcane Bagasse Ash (SBA), a fibrous residue generated as a by-product of the sugar industry after juice extraction and bagasse combustion, has emerged as a promising material for sustainable construction. As sugarcane is one of the world's largest cultivated crops, SBA is abundantly available in agricultural economies, such as Nigeria, Ethiopia, and Malaysia. Traditionally disposed of as waste or used as low-value biofuel and fertilizer, SBA has recently gained attention as a pozzolanic material rich in silica and alumina with the potential to enhance the structural performance of asphalt and concrete composites [29–32].

Previous studies have demonstrated that SBA can be used as a partial cement substitute for concrete and as a minor filler additive in bituminous mixtures, with findings suggesting potential improvements in the Marshall stability, reduced flow values, and acceptable void characteristics when used in small percentages [33,34]. However, comprehensive investigations on the use of SBA as a partial replacement for fine aggregates in HMA remain limited, particularly those concerning the effects of incremental replacement levels and consistent mix design parameters. Moreover, most existing studies vary significantly in methodology, material characterization, and substitution ratios, making it difficult to draw generalized conclusions or establish practical guidelines for large-scale implementation [35,36].

Numerous studies have been conducted outside Sub-Saharan Africa, despite the region's high sugarcane production and pressing need for low-cost, sustainable road construction solutions. In countries such as Nigeria and Ethiopia, where road infrastructure is expanding rapidly amid resource constraints, the use of SBA in HMA could yield dual benefits: mitigating environmental pollution from agricultural waste and reducing dependence on expensive imported materials. Nonetheless, the lack of localized, systematic research in these contexts constitutes a critical gap in both the academic literature and practical engineering applications [37]. In addition to addressing environmental concerns, there is a growing need to enhance the mechanical performance and durability of asphalt pavement under severe traffic and climatic conditions [38]. Common pavement failures, such as rutting, fatigue cracking, and moisture-induced damage, compromise road safety and increase maintenance costs [35,36]. Studies have shown that the modification of asphalt mixtures with natural and synthetic waste materials, including coal fly ash, palm oil fuel ash, polyethylene terephthalate (PET), coir fiber, and sugarcane fiber, can enhance structural performance while contributing to sustainable development goals. For example, the incorporation of recycled PET has been found to improve rutting resistance, while natural fibers such as kenaf and coir have been shown to increase the Marshall stability by up to 9.7 %. These findings underscore the potential of waste-derived materials to simultaneously improve performance and sustainability [39–41].

Despite the growing body of research on modified asphalt mixtures and the use of alternative materials to improve performance and sustainability, there is still limited systematic investigation into the use of agricultural waste ashes, such as sugarcane bagasse ash, as partial replacements for mineral fillers in hot-mix asphalt across a comprehensive range of substitution levels. Prior work has explored various waste fillers, including coal bottom ash, which improved rutting resistance and fatigue life when used as partial filler replacements in HMA mixtures, indicating the broader potential of industrial by-products in asphalt design [42,43]. Comprehensive reviews have highlighted the benefits of waste fillers, such as fly ash, rice husk ash, and construction/demolition wastes, in enhancing the mechanical characteristics, durability, and environmental performance of asphalt mixtures while simultaneously mitigating the environmental impact [44]. Other studies have examined the effects of different waste materials (e.g., fine aggregate and mineral filler effects on permanent deformation or polymer-modified systems) on asphalt performance [38,45–47]. However, few studies have focused specifically on SBA behavior as a core structural filler substitute across incremental replacement levels, nor have they combined rigorous experimental testing with numerical modeling to validate observed mechanical trends and failure mechanisms.

In addition, the coupling of laboratory testing with numerical modeling to validate the cracking mechanisms in SBA-modified asphalt remains limited. Therefore, this study aims to bridge this gap by experimentally and numerically evaluating the effect of SBA on the sustainable performance of HMA using locally sourced Nigerian materials. Laboratory tests, including Marshall stability and indirect tensile strength (ITS) tests, were conducted to assess the mechanical and volumetric characteristics of SBA-modified mixes across replacement levels of 0–16 %. A three-dimensional finite element model of the ITS test was developed to verify the experimental results and elucidate the stress–strain distributions and failure zones. Through this integrated approach, the study identified an optimal SBA replacement range (6–10 %), offering enhanced strength, reduced air voids, and improved binder–filler interactions.

This study contributes to the existing body of knowledge in three main ways: (i)Local Context and Material Relevance: It represents one of the first comprehensive investigations of SBA-modified asphalt using locally sourced Nigerian aggregates and bitumen, providing region-specific data for sustainable road construction in sub-Saharan Africa.(ii) Integrated Experimental–Numerical Framework: It combines laboratory testing with 3D FEM simulation of the ITS test, achieving close agreement between the predicted and measured tensile stresses. (iii) Actionable Optimal Range: It establishes a quantitative, field-applicable SBA replacement window that enhances Marshall stability, stiffness, and compaction while maintaining standard volumetric requirements.

The significance of this research lies in demonstrating the feasible, environmentally beneficial, and performance-optimized use of SBA as a filler substitute for HMA. By combining experimental and FEM validations within a local Nigerian context, this study provides a replicable framework for sustainable pavement material design in developing economies, supporting global efforts toward low-carbon and circular construction practices.

2. Materials and methods

This study adopted an integrated experimental–numerical methodology to evaluate the influence of Sugarcane Bagasse Ash (SBA) on the sustainable mechanical, volumetric, and tensile performance of hot-mix asphalt (HMA). The methodology was designed to (i) assess SBA as an alternative mineral filler using laboratory testing, and (ii) validate observed mechanical trends through finite element modeling (FEM). The overall research framework is illustrated in Fig. 1.

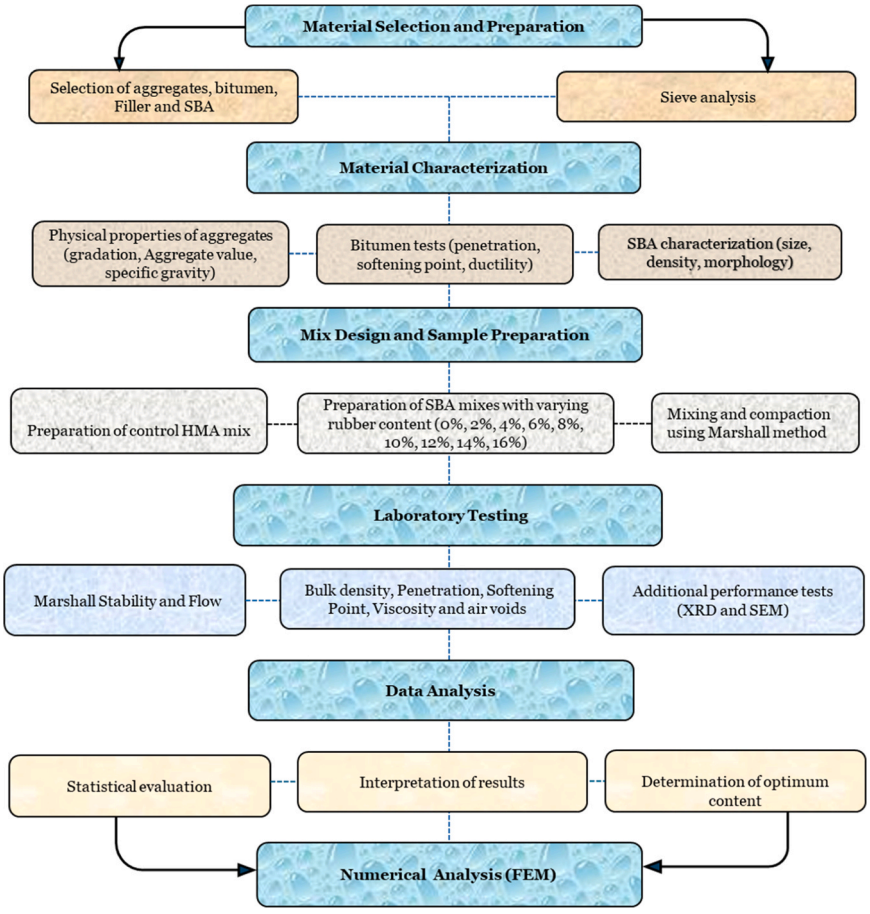

Fig. 1. Flow chart showing the Research framework for SBA Modified Hot-Mix Asphalt Mixtures.

2.1. Raw materials

This study utilized locally sourced materials that are commonly employed in asphalt pavement construction in Nigeria to ensure practical relevance and applicability. The raw materials consisted of coarse aggregates, fine aggregates, conventional mineral fillers, Sugarcane Bagasse Ash (SBA), and paving-grade bitumen. All materials were characterized in accordance with the relevant ASTM standards prior to mix preparation as illustrated in Fig. 2.

2.1.1. Bitumen

In this study, the 60/70 penetration-grade bitumen was selected because it represents the most commonly used paving-grade binder in tropical climates, such as Nigeria, where ambient temperatures often range between 25 °C and 40 °C. This grade provides an optimal balance between stiffness and flexibility, offering adequate resistance to rutting at high service temperatures, while maintaining sufficient ductility to prevent thermal cracking. To verify the temperature susceptibility of the binder, viscosity–temperature relationships were established according to ASTM D4402/D4402M. [48] The penetration index (PI) was computed from the softening point and penetration values according to the standard correlation (Eqs. (1) and (2)). The resulting PI value of + 0.8 indicates moderate temperature susceptibility, is suitable for hot-climate asphalt pavements. This aligns with prior studies [49,50] reporting that 60/70 penetration-grade bitumen performs optimally under the warm environmental conditions typical of West Africa.

$$PI = \frac{20 - 500A}{1 + 50A} \tag{1}$$

$$A = \frac{\log\left(P_2/P_1\right)}{T_2 - T_1} \tag{2}$$

Where P_1, P_2 are penetration values at temperatures T_1, T_2, respectively.

2.1.2. Coarse aggregate

The coarse aggregates used in this study were granite-based and conformed to the size requirements that are typically applied in asphalt concrete production. The aggregate sizes ranged from 6.3 mm (minimum) to 12.5 mm (maximum), following the standard gradation for dense-graded asphalt mixtures. Granite was sourced from the Royal Quarry Construction, located in Abeokuta, Ogun State, Nigeria. The specific gravity of the aggregate was measured as 2.65, which is within the standard range for crushed granite used in pavement applications. Chemical analysis of the granite was performed to evaluate its mineralogical composition, which is critical for assessing aggregate-binder adhesion, durability, and reactivity.

2.1.3. Fine aggregate

The fine aggregates used in this study were natural sand and crushed granite fines, which were selected based on their availability

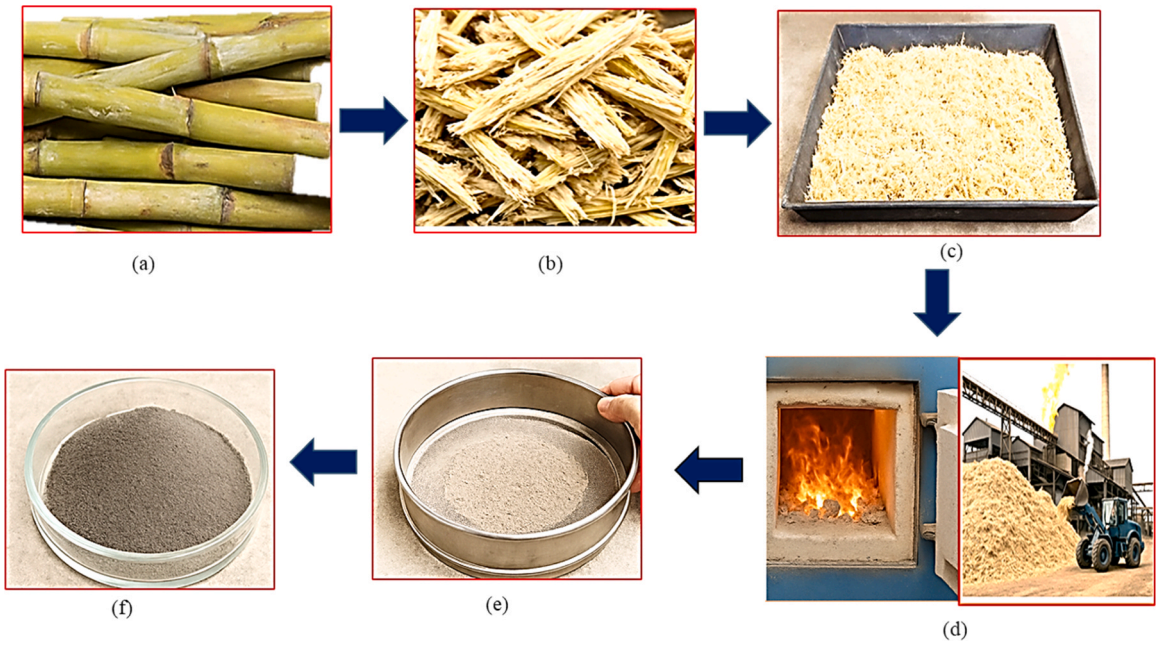

Fig. 2. Production process of Sugarcane Bagasse Ash (SBA) for Hot-Mix Asphalt (HMA), showing (a) sugarcane feedstock, (b) Sugarcane straw; (c) bagasse drying; (d) combustion at 650 °C for 3 h; (e) sieving to < 75 μm and (f) pre-treated SBA ready for mixing.

and compatibility with asphalt. The particle size distribution ranged from 4.75 mm (maximum) to 75 μm (minimum), which is consistent with the specifications for mineral fillers and fine aggregates in hot mix asphalt (HMA).

2.1.4. Conventional mineral filler

The conventional mineral filler was quarry-derived limestone dust passing a 0.075 mm (No. 200) sieve. Mineral fillers play a critical role in asphalt mixtures by filling microvoids, stiffening the asphalt mastic, and enhancing the aggregate–binder interaction. The limestone filler used in the control mixture was employed without chemical modification and served as the reference filler, against which the performance of the SBA-modified mixtures was evaluated.

2.1.5. Sugarcane bagasse ash (SBA)

Sugarcane Bagasse Ash (SBA) was used as a partial replacement for the conventional mineral fillers. Raw sugarcane bagasse was sourced from a local sugar-processing facility and was subjected to controlled combustion to obtain ash with suitable physicochemical characteristics. The bagasse was air-dried and combusted in a muffle furnace at 650 ± 10 °C for 3 h, a temperature selected to ensure complete removal of organic matter while preserving amorphous silica phases. After cooling, the ash was lightly ground and sieved to pass through a 0.075 mm sieve, producing a fine filler fraction compatible with asphalt mixtures. The processed SBA exhibited low bulk density and porous particle morphology. Chemical analysis showed that SBA is rich in silica (SiO_2), with minor amounts of alumina (Al_2O_3), calcium oxide (CaO), and iron oxide (Fe_2O_3). These characteristics suggest that SBA can act not only as a physical filler but also as a reactive component that enhances binder–filler interactions and mixture densification when used at appropriate replacement levels.

2.2. SBA production and pre-treatment parameters

Raw sugarcane bagasse was collected from a local sugar-processing facility and air-dried for 48 h to remove surface moisture and to reduce the likelihood of incomplete combustion. The dried bagasse was subsequently combusted in a laboratory muffle furnace at 650 ± 10 °C for 3 h. The selected combustion temperature and duration were based on previous optimization studies [29–32], ensuring high amorphous silica content and minimal crystalline formation. The resulting SBA exhibited light-gray coloration, low bulk density, and porous surface morphology, features consistent with pozzolanic and reactive ash suitable for use in Hot-Mix Asphalt. After combustion, the ash was allowed to cool naturally to the ambient temperature to prevent thermal shock and particle agglomeration. The cooled material was then lightly ground to break down the agglomerates without significantly altering the particle morphology and sieved through a 0.075 mm (No. 200) sieve in accordance with ASTM C136 [51]. This process produced a fine filler fraction that was compatible with the conventional mineral fillers used in asphalt mixtures. Laser diffraction analysis showed that the processed SBA particles ranged from approximately 1 μm to 75 μm, with a median particle size (D_{50}) of about 32 μm.

The processed SBA exhibited a low bulk density and porous, irregular particle morphology, resulting in a high specific surface area. These characteristics enhance the physical adsorption of the asphalt binder and promote stronger filler–binder interactions, leading to improved mechanical stiffness and mixture densification at moderate replacement levels. In addition, the silica-rich and predominantly amorphous composition of SBA, confirmed by XRD and EDX analyses, contributes to increased surface activity, further strengthening the binder–filler interactions.

However, owing to its low density and porous nature, excessive incorporation of SBA may reduce packing efficiency and increase binder demand, resulting in overfilling effects and reduced mechanical performance. This behavior explains the deterioration observed at higher SBA replacement levels (> 10 %) in the experimental results. Therefore, controlling both the preparation conditions and dosage of SBA is essential for achieving optimal performance in SBA-modified hot-mix asphalt.

2.3. Testing methods and statistical treatment

All laboratory tests (Fig. 3) conducted in this study were performed in accordance with the relevant ASTM standards to ensure

(a) (b) (c)

Fig. 3. (a). Penetration test; (b) weighing of asphalt (c) water absorption.

repeatability, reliability, and comparability with existing literature. To account for experimental variability, each mechanical and volumetric test was performed on a minimum of three replicate specimens for each SBA replacement level. The reported results represent the mean values of the replicates. Where applicable, standard deviations were calculated and used to assess the data dispersion and consistency.

2.3.1. Sieve analysis

The specific gravities of fine and coarse aggregates typically lie between 2.61 and 2.64. Aggregates used in construction typically have specific gravities between 2.5 and 3.0, with an average of 2.68. The aggregates have a specific gravity of 2.65. Most of the aggregates employed in this study had diameters of 9.5–12.5 mm. The specific gravity value of 2.65, which is close to the average specific gravity value of 2.68 and is within the range of 2.5–3.0 described in ASTM D70 [52]. The specific gravity or relative density of the aggregate was calculated by dividing its weight by an equivalent amount of water. The specific gravity of each sample, excluding any potentially permeable spaces, reflected the density of its constituent components. The mechanical strength of such materials can easily be correlated with a specific gravity value, making them an important element in the assessment and identification of aggregates used in engineering construction. This involved determination of the particle size distribution of fine and coarse aggregates by sieving. This test method was used primarily to determine the grading of materials proposed for use as aggregates or used as aggregates. The results were used to determine the compliance of the particle size distribution with the applicable specification requirements and to provide the necessary data for controlling the production of various aggregate-containing products and mixtures. The data may also be useful for developing relationships between the porosity and packing. The accurate determination of materials finer than the 75-μm (No. 200) sieve cannot be achieved using this test method alone. The tests were performed in accordance with standards ASTM C136 [51].

2.3.2. Elongation index test

The elongation index (EI) represents the percentage of aggregate particles whose length exceeds 1.8 times their mean dimension and applies to aggregates retained on a 6.3 mm sieve, as specified in ASTM D4791 [53]. The *EI* was calculated as the ratio of the mass of elongated particles to the total test mass. This test does not apply to materials passing the 6.3 mm sieve or retained on a 50 mm sieve. Aggregates are generally considered unsuitable if the *EI* exceeds 45 %, while several standards, including BS 1241 and Indian Standard specifications, recommend a maximum *EI* of 30 %. In this study, the measured EI was 25 %, which is within the acceptable limit and indicates suitability for use in asphalt cement concrete and other pavement layers. The elongation index provides insight into aggregate shape and particle packing characteristics. The *EI* was calculated using the formula presented in Eq. (3).

$$EI(\%) = \frac{Mass\ of\ elongated\ particles}{Total\ mass\ of\ sample} x \quad 100 \tag{3}$$

2.3.3. Flakiness index test

The flakiness index (FI) measures the percentage of aggregate particles whose thickness is less than 0.6 times their mean diameter. Aggregates with high flakiness are generally undesirable for road construction, particularly for surface layers. According to ASTM C131 [54], the flakiness index for road aggregates should not exceed 30 %. The flakiness index was calculated as the ratio of the mass of flaky particles to the total sample mass. Each size fraction was measured using a thickness gauge, and the weights of flaky particles were recorded. Aggregate shape is a critical factor influencing the performance of bituminous mixes, as flaky particles tend to pack more closely and reduce void content, thereby affecting binder demand. In this study, the flakiness index was found to be 29 %, which is within the permissible limit and therefore suitable for pavement construction. The flakiness index was calculated using the formula provided in Eq. (4).

$$FI(\%) = \frac{Mass\ of\ flaky\ particles}{Total\ mass\ of\ sample} x \quad 100 \tag{4}$$

2.3.4. Los Angelis abrasion

The Los Angeles Abrasion (LAA) test was used to evaluate the resistance of aggregates to abrasion and impact, which simulates the wear experienced by pavement aggregates under traffic loading. The test measures aggregate degradation caused by abrasion and impact in a rotating steel drum containing steel balls. Aggregates used in highway pavements are subject to continuous abrasion from vehicular traffic, making abrasion resistance a critical property for pavement performance. In this study, the LAA value of the aggregates was 24.8 %, which is within the maximum allowable limit of 30 % for road construction aggregates. This indicates that the aggregates are suitable for use in hot mix asphalt (HMA) and other pavement layers. The test was conducted in accordance with ASTM C131 [54] and the abrasion value was calculated using the formula presented in Eq. (5).

$$LAA(\%) = \frac{W_{original} - W_{retained}}{W_{original}} \times 100 \tag{5}$$

2.3.5. Aggregate impact value (AIV) analysis

When employed as a wear course for pavements, the aggregate impact should not exceed 30 %. The maximum values were 35 % for bituminous macadam and water-bound macadam (WBM) base courses. The tested aggregate's AIV value of 20.9 % obtained in this study is satisfactory and suitable for use as a road building aggregate and is in line with the specified 25 % maximum in Eq. (6).

$$\text{AIV}(\%) = \left(\frac{\text{Weight of fines(passing2.36mm sieve}}{\text{Total weight of sample}}\right) \times 100 \quad (6)$$

2.3.6. Specific gravity

The mass of a particular volume of the bituminous material was divided by the mass of an equal volume of water at 27 °C to obtain the specific gravity of the bituminous material. The bitumen sample was placed in a calibrated pycnometer as a part of the process. The residual volume was filled with water after weighing the pycnometer and sample. The filled pycnometer was heated to the test temperature and then weighed in a liquid bath. The mass of the sample and mass of water displaced by the sample in the filled pycnometer were used to compute the density. The test was performed in accordance with the ASTM D70 [52] standard and the formula for the analysis, as shown in Eq. (7).

Bulk Specific Gravity of Mix (G_{mb}).

$$G_{mb} = \frac{W_d}{V} \quad (7)$$

Where W_d = Dry weight of the compacted specimen (g) and V = Volume of the specimen (cm^3).

2.3.7. Penetration testing

The penetration test is a widely adopted empirical method for characterizing the consistency of bitumen, particularly its hardness or softness, under standard conditions. The test involves measuring the vertical distance, expressed in tenths of a millimeter (0.1 mm), that a standard needle penetrates a bitumen sample under a fixed load of 100 g, maintained for 5 s at a controlled temperature of 25 ± 0.1 °C. The penetration depth indicates the relative hardness of the bitumen; a higher penetration value corresponds to softer bitumen, whereas a lower value indicates a harder grade. This test was performed in accordance with international standards such as ASTM D5, [55] and is primarily used for the classification and grading of bitumen for paving applications. Although simple and cost-effective, the penetration test has limitations, including the inability to provide rheological data or performance-related parameters over a wide range of service temperatures. However, it remains a fundamental quality-control tool for testing bituminous materials.

2.3.8. Marshall testing

The Marshall Stability test is a standardized and widely adopted method for evaluating the mechanical performance and volumetric properties of asphalt mixtures. In this study, a test was conducted to assess the influence of Sugarcane Bagasse Ash (SBA) on the stability, flow, and overall structural behavior of asphalt concrete. The primary objective was to determine the optimal SBA content to enhance the performance characteristics of the mixture, while maintaining or improving its durability and workability. Asphalt specimens with various SBA contents (0 %, 4 %, 8 %, 12 %, and 16 % by weight of filler) were prepared and subjected to the Marshall Stability test, as shown in Fig. 4. The volumetric parameters are shown in Eqs. (8)–(11).

$$\text{A V}(\ \%\ ) = \left(\frac{G_{mm-G_{mb}}}{G_{mb}}\right) \text{x}100 \quad (8)$$

$$\text{VMA}(\ \%\ ) = 100 - \left(\frac{G_{mm-P_s}}{G_{ab}}\right) \text{x}100 \quad (9)$$

$$\text{VFB}(\ \%\ ) = \left(\frac{VMA - AV}{VMA}\right) \text{x}100 \quad (10)$$

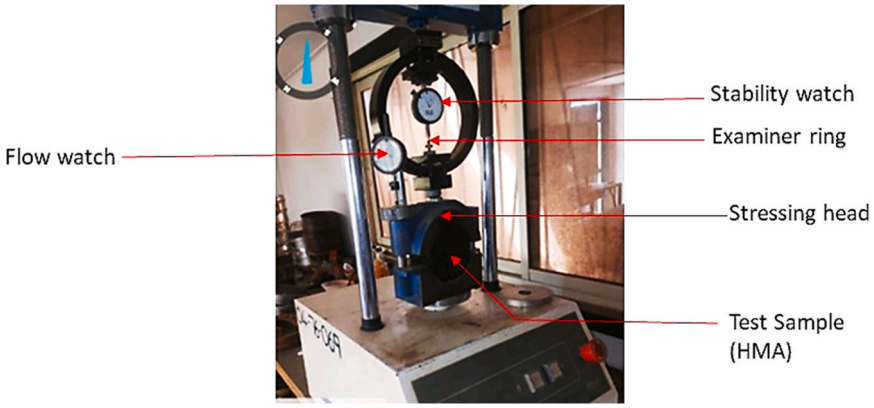

Fig. 4. Marshall testing of modified SBA asphalt mixture.

$$MQ = \left(\frac{Marshall\ Stability}{flow}\right) \tag{11}$$

2.3.9. Indirect tensile test

The Indirect Tensile Strength (ITS) test (Fig. 5) was employed to evaluate the tensile resistance of asphalt mixtures modified with Sugarcane Bagasse Ash (SBA), in accordance with the ASTM D6926 [56] guidelines. This method is widely used to assess the potential of asphalt mixtures to resist cracking and fatigue failure, particularly under the tensile stresses induced by traffic loading and thermal contraction. A compressive load was applied along the vertical diameter of cylindrical asphalt specimens. This loading configuration induced horizontal tensile stress perpendicular to the applied load. As the load increases, the tensile stress builds up at the center of the specimen until failure occurs by splitting. The maximum load at failure was used to compute the indirect tensile strength, which provides a measure of the ability of a material to withstand cracking. Cylindrical samples were prepared with a diameter of 100 mm and a height of 63.5 mm, compacted using the Marshall method with 75 blows per face. The specimens were produced by replacing the conventional mineral fillers with SBA at various concentrations (0–16 %). The specimens were conditioned at 25 ± 1 °C for at least 24 h prior to testing to ensure uniform temperature distribution.

The prepared sample was positioned horizontally in the loading frame, with a loading strip on both the top and bottom contact points. A compressive load was applied along the vertical plane at a constant deformation rate of 50 mm/min until failure occurred via diametral splitting. The maximum load (P) at failure was recorded. Tensile Strength The indirect tensile strength (σ_t) was computed using Eq. (12)–(15):

$$\sigma_t = \frac{2P}{\pi tD} \tag{12}$$

$$\sigma_t = \frac{E}{1-\nu^2}(\varepsilon_x + \nu\varepsilon_y) \tag{13}$$

$$\varepsilon_x = \frac{1}{E}(\sigma_x - \nu\sigma_y) \tag{14}$$

$$\varepsilon_y = \frac{1}{E}(\sigma_y - \nu\sigma_x) \tag{15}$$

where σ_t= indirect tensile strength (MPa); P = Maximum applied load at failure (N); t is the thickness of the specimen (mm); D = Diameter of the specimen (mm); π = 3.1416; ε_x is the horizontal (induced tensile) strain; ε_y is the vertical (compressive) strain. This equation assumes a uniform stress distribution along the loading plane and is valid for cylindrical specimens with standard proportions. The ITS test provides a reliable, indirect measurement of the asphalt mixture's tensile cracking resistance, which is critical for fatigue performance under repeated loading, resistance to thermal cracking, particularly in colder climates, and durability, particularly when evaluating the effects of filler modification using waste materials such as SBA. This method also lays the foundation for more advanced evaluations such as moisture susceptibility tests, in which the Tensile Strength Ratio (TSR) can be calculated using conditioned and unconditioned samples.

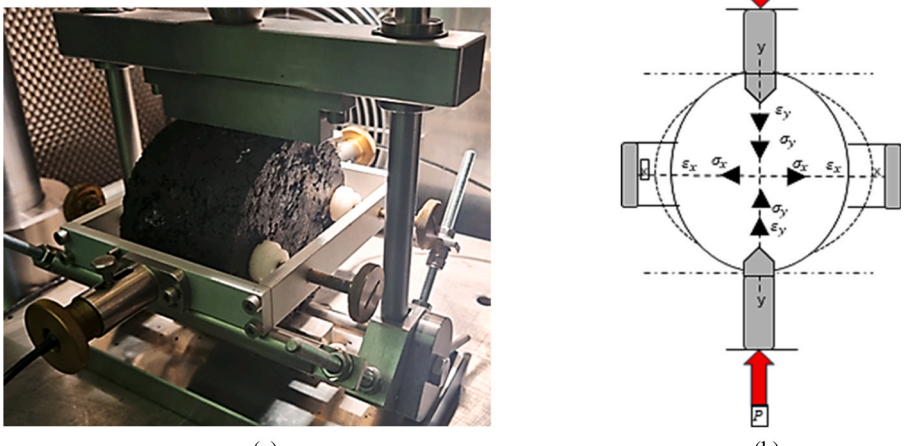

(a) (b)

Fig. 5. Indirect tensile stress (ITS) testing of modified SBA asphalt mixture: (a). Pictorial view (b). Schematic view.

3. Results and discussions

In-depth laboratory studies were conducted to explore the effects of sugarcane bagasse ash (SBA) on the engineering qualities of asphalt-mix samples. The results are presented in this section along with their interpretations and related analyses. Tables and graphs were used to portray the data after analysis. Inferential statistics were used to assess the engineering properties of the asphalt mix containing SBA. The maximum specific gravity, bulk specific gravity, Marshall stability, flow, Marshall quotient, air voids, voids in mineral aggregates, and voids filled with bitumen were obtained from Marshall stability tests conducted on asphalt samples with varying SBA inclusions. The asphalt mix proportion and test results for sugarcane bagasse ash (SBA) as a partial replacement of filler content in the asphalt mixture at various percentages, including 0 %, 2 %, 4 %, 6 %, 8 %, 10 %, 12 %, 14 %, and 16 % by weight of filler.

3.1. Physical and chemical properties of bitumen

The physical and chemical properties of the 60/70 penetration grade bitumen used in this study complied with national specifications and ASTM standards, as summarized in Table 1. The results confirm its suitability for flexible pavement construction. The bitumen exhibited a solubility of 99 % in carbon disulfide (CS_2), meeting the ASTM D2042 [57] requirement and indicating high purity with negligible non-bituminous impurities. The penetration value was 60 mm, which lies within the specified 60–70 mm range and classifies the binder as moderately hard, making it suitable for use in hot climatic conditions due to its resistance to deformation. The specific gravity was measured at 1.03, falling within the acceptable range of 1.01–1.06 [52], and ensuring compatibility with standard asphalt mix design requirements.

The softening point was 47 °C, slightly below the recommended range of 48–56 °C [58], suggesting marginally lower thermal resistance that may require consideration in high-temperature environments. The flash point was 247 °C, exceeding the minimum safety requirement of 232 °C [59], confirming safe handling and application during asphalt production.

Chemical analysis (Table 2) revealed that the bitumen was predominantly composed of carbon (82 %) and hydrogen (10 %), confirming its hydrocarbon nature. Minor elements such as sulfur (4 %), nitrogen (1 %), and oxygen (1.5 %) were also present, which is typical of petroleum-derived bitumen. Trace amounts of metals, including nickel (Ni) and vanadium (V), were detected, likely originated from the crude oil source. When present in small quantities, these elements may influence the aging and oxidative stability of the binder over time. The physical and chemical properties of the 60/70 penetration-grade bitumen samples are largely compliant with ASTM and national standards. The material demonstrated sufficient purity, thermal stability, and consistency for use in flexible pavement constructions. The slight deviation in softening point warrants further investigation, particularly if the material is intended for use in environments with high surface temperatures. Nonetheless, bitumen samples were deemed suitable for standard road construction applications

3.2. Physical and chemical properties of aggregate

The physical and chemical characteristics of the aggregates used in this study were evaluated to confirm their suitability for hot-mix asphalt (HMA) production. Aggregate quality is a critical factor governing the strength, durability, and deformation resistance of asphalt mixtures, as it directly affects interlocking, load transfer, and binder adhesion.

3.2.1. Aggregate gradation

The gradation of the aggregates used for the hot mix asphalt (HMA) design was evaluated using standard sieve analysis, and the results are illustrated in Fig. 6. Aggregate gradation is a critical factor that influences the mechanical behavior, workability, and durability of asphalt mixtures. The particle size distribution not only affects the density and void content but also significantly influences the stability and resistance to deformation under traffic loads. The sieve analysis results indicate that the aggregate gradation complied with the standard requirements specified in ASTM D6913 [60]. For instance, the percentage passing through the 12.5 mm sieve is 95 %, which falls within the recommended range of 85–100 %. Similarly, the percentage passing for the finer sieves such as 2.36 mm (48 %) and 0.075 mm (7 %) also lies within their respective specified ranges (36–51 % and 5–8 %). This indicates that the aggregate blend possesses a well-graded structure, which is desirable for achieving optimal packing density and reduced voids in the mix. The gradation curve further confirms the continuous and dense grading, suggesting that the selected aggregate blend is suitable for producing a stable and durable asphalt mix. Appropriate gradation ensures the good interlocking of particles, which is crucial for

Table 1
Physical properties of 60/70 Pen. Bitumen.

Property	Result	Recommended Specification	American Standard	Recommended Specification
Solubility (%)	99	99	ASTM D2042 [57]	99
Penetration (mm)	60	60 – 70	ASTM D5 [55]	60–70
Specific Gravity	1.03	1.01 – 1.06	ASTM D70/D70M [52]	1.01–1.06
Softening Point at 60 °C (°C)	47	48–56	ASTM D36 [58]	49–56
Flash point °C	247	225–250	ASTM D36 [58] ASTM D92 [59]	232–250

Table 2
Chemical characteristics of bitumen (60/70 penetration grade).

Component	Typical Proportion (%)
Carbon (C)	82
Hydrogen (H)	10
Sulfur (S)	4
Nitrogen (N)	1
Oxygen (O)	1.5
Metals (Ni, V)	Trace

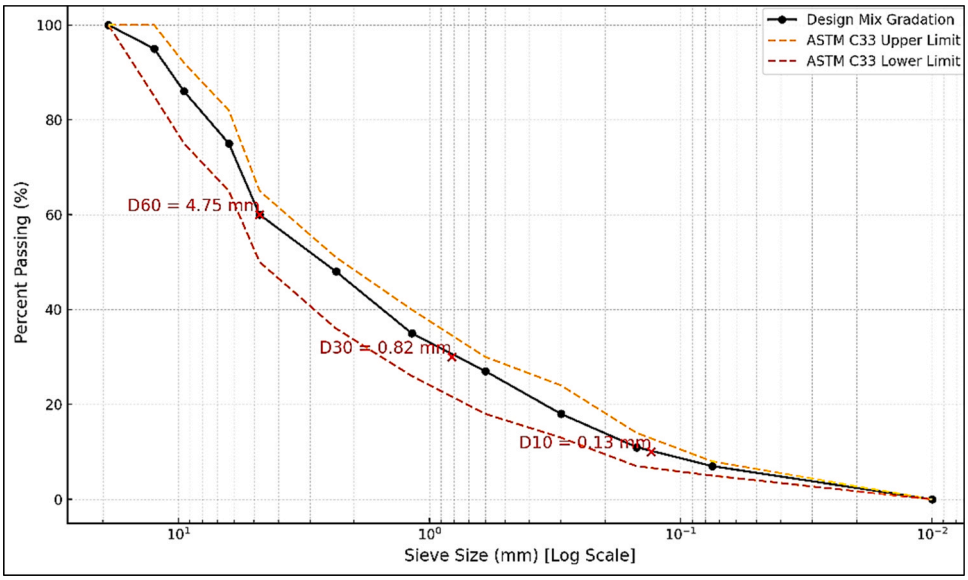

Fig. 6. Gradation curve of aggregates for design mix of HMA.

the load-bearing performance of pavements.

3.2.2. *Physical properties of aggregates*

Table 3 summarizes the key physical properties of the coarse and fine aggregates used in this study. The granite-based coarse aggregate exhibited a bulk specific gravity of 2.65, which is within the typical range (2.5–3.0) specified for pavement aggregates. The low water absorption value (0.8 %) indicates minimal porosity and good durability.

The Los Angeles Abrasion (LAA) value of 24.8 % is below the maximum allowable limit of 30 % for asphalt surface courses, confirming adequate resistance to abrasion and impact under traffic loading. Similarly, the Aggregate Impact Value (AIV) of 20.9 % satisfies the recommended limit ($\leq$ 25 %), indicating good toughness and suitability for flexible pavement applications. The flakiness and elongation indices were also within permissible limits, suggesting that the aggregates possess a predominantly cubical shape, which enhances packing efficiency and mechanical interlock in asphalt mixtures.

Table 3
Physical properties of materials used in the study.

Material	Property	Test Standard	Value	Specification/Limit
Coarse Aggregate (Granite)	Nominal size (mm)	ASTM C136 [51]	6.3–12.5	—
	Bulk specific gravity	ASTM C127 [61]	2.65	2.5–3.0
	SSD specific gravity	ASTM C127 [61]	2.67	—
	Water absorption (%)	ASTM C127 [61]	0.8	$\leq$ 2.0
	Los Angeles abrasion (%)	ASTM C131 [54]	24.8	$\leq$ 30
	Aggregate impact value (%)	ASTM C131 [54]	20.9	$\leq$ 25
Fine Aggregate	Maximum size (mm)	ASTM C136 [51]	4.75	—
	Bulk specific gravity	ASTM C128 [62]	2.62	2.5–3.0
	Water absorption (%)	ASTM C128 [62]	1.2	$\leq$ 3.0
Conventional Filler (Limestone)	Passing 0.075 mm (%)	ASTM C136 [51]	100	$\geq$ 95

3.2.3. Chemical composition of aggregates

The chemical compositions of the granite-based coarse aggregates are listed in Table 4. The predominant oxide identified was silicon dioxide (SiO_2) at 68 %, which is characteristic of siliceous aggregates, such as granite. High silica content is indicative of aggregates with good hardness and abrasion resistance, making them suitable for high-traffic pavement applications. Aluminum oxide (Al_2O_3) and potassium oxide (K_2O) were recorded at 14 % and 5 %, respectively. These compounds are typically associated with feldspar minerals present in granite. Their presence may slightly influence the thermal expansion behavior of the aggregates but generally does not pose issues in asphalt mixtures.

Minor oxides, such as sodium oxide (Na_2O) (3 %) and calcium oxide (CaO) (2 %) were also detected. While a high CaO content can lead to stripping problems in asphalt mixes, the observed concentration is low enough not to adversely affect moisture susceptibility. Iron oxide (Fe_2O_3) at 2 % and trace levels of magnesium oxide (MgO) and titanium dioxide (TiO_2) (< 1 %) were also present. These oxides are typical of igneous rock-derived aggregates and have a minimal negative impact on asphalt performance. The loss on ignition (LOI) was less than 1 %, indicating a low organic or volatile content and confirming the mineralogical stability of the aggregates. The combination of favorable gradation and stable chemical composition confirmed the suitability of the tested aggregates for use in HMA. A well-graded nature ensures a dense and stable mix, whereas chemical stability and mineral hardness suggest good performance under traffic and environmental loading conditions. These findings are consistent with the requirements of high-quality aggregate materials for flexible pavement construction.

3.3. Characterization of modified SBA hot mix asphalt

3.3.1. Mix proportioning for modified SBA hot mix asphalt

The mix proportioning in this study followed the Marshall mix design procedure in accordance with ASTM D6926 [56]. Control hot-mix asphalt (HMA) was designed using granite-based coarse and fine aggregates with a conventional mineral filler. The optimum asphalt binder content was determined to be 5.1 % by the total mix weight, providing a reference for all modified mixes. In the modified mixes, Sugarcane Bagasse Ash (SBA) was introduced as a partial replacement for the conventional mineral fillers. SBA was incorporated at incremental replacement levels of 2 %, 4 %, 6 %, 8 %, 10 %, 12 %, 14 %, and 16 % of filler weight. All other mix constituents — aggregate gradation, asphalt binder content, and compaction energy — were kept constant to isolate the effect of the SBA content on the mix behavior. The aggregates used in this study conformed to ASTM C136 [51] gradation standards and had a specific gravity of 2.65. The asphalt cement used was penetration-grade 60/70 bitumen compliant with ASTM D946 [63]. A consistent mixing temperature of 160 ± 5 °C and compaction temperature of 150 ± 5°C were maintained for all batches. Each mix was prepared and compacted using 75 blows per face in a Marshall compaction mold and subjected to standard volumetric and mechanical testing. These include the bulk specific gravity (G_{mb}), maximum specific gravity (G_{mm}), stability, flow, air voids, and Marshall quotient (MQ). Tables 5 and 6 summarize the key Mix Proportions of Materials Used in Control and SBA-Modified Asphalt Mixtures and the chemical composition of SBA, respectively.

3.4. Volumetric analysis

The Marshall Stability, a critical indicator of resistance to plastic deformation underload, increased with the inclusion of up to 8 % SBA, peaking at 9.0 kN. This enhancement suggests an improved aggregate-binder interaction and filler effect owing to the finer particles of SBA, which may have contributed to the denser matrix. However, a further increase in SBA beyond 10 % resulted in a gradual decline in stability, with 6.2 kN recorded at 16 % SBA. This reduction may be attributed to excessive ash interfering with proper binder coating and interparticle bonding, leading to potential brittleness or reduced cohesion. The formula used for analyzing the different parameters in the Marshall stability test is shown in Eq. (9)–(12). The Marshall Quotient (MQ), which represents the stiffness of the mixture (stability/flow), followed a similar trend. An MQ increase from 3.0 kN/mm (at 0 % SBA) to 3.3 kN/mm (at 6 %–10 % SBA) indicates a stiffer and more rut-resistant mixture within this range. However, the MQ values began to decline at higher SBA content, reinforcing the notion of diminishing returns past the optimal range. In terms of volumetric properties, the bulk density steadily increased from 2.42 g/cm^3 to 2.51 g/cm^3 as SBA content reached 8 %, before tapering slightly. This reflects improved particle packing and reduced void content up to a certain threshold, after which an excessive filler content may hinder compaction. Conversely, the air void content decreased significantly from 4.9 % (0 % SBA) to 3.5 % (6–10 % SBA), implying improved densification and

Table 4
Chemical composition of coarse aggregate (granite-based).

Oxide/Compound	Typical Range (% by weight)
Silicon Dioxide (SiO_2)	68
Aluminum Oxide (Al_2O_3)	14
Potassium Oxide (K_2O)	5
Sodium Oxide (Na_2O)	3
Calcium Oxide (CaO)	2
Iron Oxide (Fe_2O_3)	2
Magnesium Oxide (MgO)	< 1
Titanium Dioxide (TiO_2)	< 1
Loss on Ignition (LOI)	< 1

Table 5
Mix proportions of materials used in control and SBA-modified asphalt mixtures.

Material	Proportion (% by Total Mix Weight)
Coarse Aggregate	40
Fine Aggregate	45
Mineral Filler (SBA)	0 %,2 %,4 %,6 %,8 %,10 %, 12 %,14 %,16 %.
Conventional Filler	15 → decreasing with SBA addition
Asphalt Binder (Bitumen)	5.1

Table 6
Chemical composition of sugarcane bagasse ash (SBA).

Oxide	Typical Composition (%)
Silicon dioxide (SiO_2)	65
Aluminum oxide (Al_2O_3)	6
Ferric oxide (Fe_2O_3)	4.5
Calcium oxide (CaO)	6.5
Magnesium oxide (MgO)	3
Sodium oxide (Na_2O)	< 1
Potassium oxide (K_2O)	3
Loss on ignition (LOI)	10

reduced permeability. These values fall within the acceptable range (3–5 %) for asphalt mix design, ensuring durability without compromising fatigue resistance. Table 7 presents the volumetric analyses of sugarcane bagasse ash (SBA) and asphalt at different percentages.

The Voids in Mineral Aggregate (VMA) initially decreased with increasing SBA content, reached a minimum at 8 %, and then increased again to 10 %. While the VMA values remained within the standard range (10–15 %), the lowest VMA at 8 % SBA implied optimal particle arrangement and void filling. Simultaneously, the Voids Filled with Bitumen (VFB) increased with the SBA content, peaking at 72 % (14 % SBA), which suggests higher bitumen retention and potentially better moisture resistance. However, an excessively high VFB can also result in bleeding and reduced air voids, compromising structural performance over time. The results indicate that the optimal SBA replacement level lies within the 6–10 % range, where a balance is achieved between strength, stiffness, density, and durability. Specifically, 8 % SBA offers the most promising enhancement in terms of the Marshall Stability, MQ, and volumetric parameters without adversely affecting the mixing behavior. Beyond this range, adverse effects such as reduced strength, lower stiffness, and poor compaction are shown in Fig. 7(a)–(h).

3.4.1. Effect of sugarcane bagasse ash (SBA) on Marshal quotient (MQ) and flow

The effect of Sugarcane Bagasse Ash (SBA) on the Marshall Quotient (MQ) and flow characteristics of asphalt mixtures is presented in Fig. 7(a–b). The addition of SBA initially increased Marshall stability due to the filler effect of its fine particles, which improved aggregate packing, inter-particle friction, and binder–filler interaction. As a result, MQ increased up to the optimum SBA content, indicating enhanced stiffness and resistance to permanent deformation. Similar improvements have been reported in previous studies where agricultural waste ashes functioned as active fillers in asphalt mixtures. Beyond the optimum SBA level, both stability and MQ decreased, likely due to excessive ash content weakening the aggregate–binder bond and increasing mixture brittleness. This decline suggests reduced durability and a higher susceptibility to cracking under repeated traffic loading. As shown in Fig. 7(b), flow values exhibited an inverse trend. Flow decreased with SBA addition to the optimum dosage, reflecting increased stiffness and improved resistance to plastic deformation. However, further SBA addition slightly increased flow values, possibly due to poor dispersion of excess ash within the binder, leading to mix heterogeneity. Maintaining flow within the recommended range is essential, as very low values may cause brittle behavior, while high values indicate rutting susceptibility. SBA can be effectively used as a partial filler

Table 7
Volumetric analysis of sugarcane bagasse ash (SBA) and asphalt at different percentages.

SBA (%)	Marshall Quotient (kN/mm)	Flow (mm)	Bulk Density (g/cm³)	Max Density (g/cm³) [Gmm]	VMA (%)	Marshall Stability (kN)	Air Void (%)	VFB (%)
0	3	2.5	2.42	2.55	13.3	7.6	4.9	63.2
2	3	2.6	2.44	2.58	12.6	7.9	5	60.3
4	3.2	2.6	2.46	2.59	11.9	8.3	4.6	61.3
6	3.3	2.7	2.5	2.59	10.5	8.8	3.5	66.6
8	3.3	2.7	2.51	2.6	10.1	9	3.5	65
10	3.3	2.6	2.48	2.57	11.2	8.6	3.5	68.7
12	3	2.5	2.45	2.55	12.2	8	3.97	68
14	2.9	2.3	2.42	2.52	14	6.7	4.4	72
16	2.7	2.3	2.4	2.49	15.4	6.2	4.4	71.4

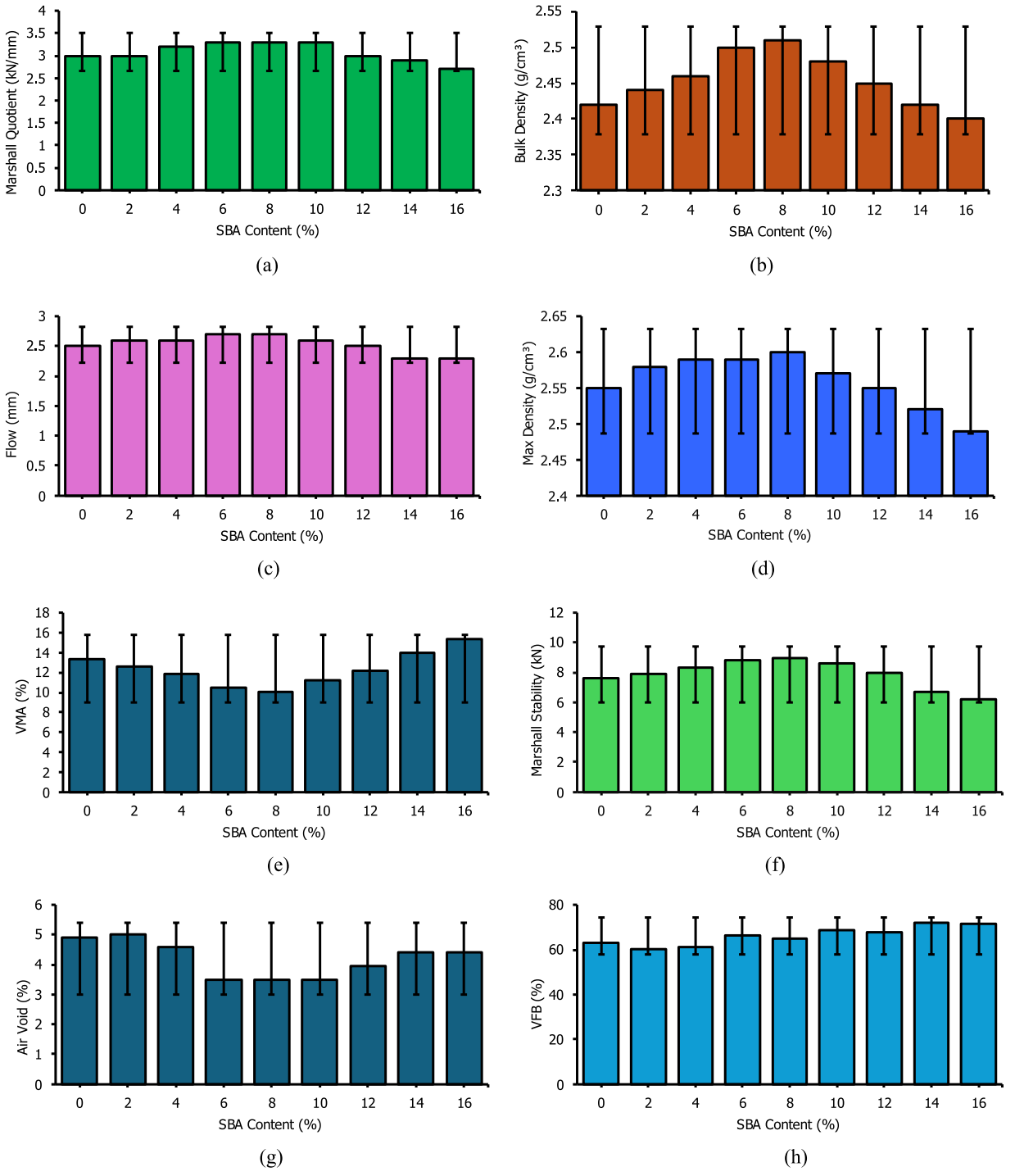

Fig. 7. Volumetric results (a). Marshall Quotient-kN/mm; (b). Bulk density-g/cm^3; (c). Flow-mm; (d). Maximum density-g/cm^3; (e). VMA%; (f). Marshall stability-kN; (g). Air void-%; (h). VFB%.

replacement in asphalt mixtures. An optimum content, typically between 4 % and 6 %, provides a balanced improvement in stability and deformation characteristics, while higher replacement levels diminish these benefits. Although SBA incorporation reduces bulk density, controlled replacement levels can maintain adequate structural performance while supporting sustainability objectives in pavement construction.

3.4.2. Effect of voids in mineral aggregate (VMA)

The effect of Sugarcane Bagasse Ash (SBA) on the voids in mineral aggregates (VMA) is illustrated in Fig. 7e. VMA is a critical volumetric parameter that governs the space available within the aggregate structure to accommodate bitumen and air voids, thereby influencing the durability and stability of asphalt mixtures. It is evident that the incorporation of SBA altered the VMA characteristics of the mix. At lower replacement levels, a slight reduction in VMA was observed, which may be attributed to the filler effect of SBA particles. Fine ash effectively occupied the microvoids between the aggregates, resulting in improved packing density. This enhances the contact between the aggregate particles and binder, contributing to the higher Marshall stability values at the optimum SBA content. VMA tended to increase at higher SBA content. This behavior can be explained by the porous and lightweight nature of SBA particles, which reduces the packing efficiency of the mix and creates additional void spaces. Consequently, the stability begins to decline beyond the optimum level because excessive voids compromise the mixture's internal cohesion and load resistance. This finding is consistent with earlier studies on the use of agricultural waste ashes in asphalt mixtures, where moderate filler replacement improved packing and strength, while excessive addition led to weakened aggregate–binder interactions. The observed relationship between the Marshall stability and SBA content indicates that there is an optimum level of ash incorporation at which VMA is minimized and stability is maximized. Beyond this point, increasing the VMA content adversely affects the structural performance of the mixture. Maintaining the VMA within the recommended range is essential to ensure durability against moisture damage, while avoiding excessive voids that reduce the load-bearing capacity.

3.4.3. Effect of SBA on air voids and voids filled with bitumen (VFB)

The effects of Sugarcane Bagasse Ash (SBA) on air voids (AV) and voids filled with bitumen (VFB) in Hot Mix Asphalt (HMA) are shown in Fig. 7(g–h). As the SBA content increased, the number of air voids decreased to the optimum replacement range, reflecting improved packing density and mixture compatibility. The values obtained remained within the recommended design range of 3–5 %, ensuring adequate durability and resistance to fatigue while minimizing permeability. In contrast, the VFB values increased with increasing SBA content, indicating enhanced binder retention and stronger filler–binder interactions. Moderate replacement levels supported better durability and moisture resistance, whereas excessive replacement ($>$ 10 %) produced a disproportionately high VFB, which may cause bleeding and reduce structural stability under traffic. Overall, the results suggest that SBA contributes to an improved balance between AV and VFB, when used in controlled amounts. The optimum performance occurred within 6–10 % SBA, aligned with the findings from the Marshall stability and density analyses.

3.4.4. Effect of sugarcane bagasse ash (SBA) on bulk density

The variation in bulk density with different proportions of Sugarcane Bagasse Ash (SBA) is presented in Fig. 8. The results indicated that the bulk density decreased progressively with increasing SBA content. This trend can be attributed to the relatively low specific gravity of SBA compared with that of conventional mineral fillers. The replacement of a portion of the mineral filler with SBA introduces lighter particles into the mix, thereby reducing the overall density of the asphalt mixture. At lower replacement levels, the reduction in the density was marginal because the ash particles occupied the voids between the aggregates and contributed to a denser packing structure. However, as the proportion of SBA increased, the lightweight nature of the ash became more dominant, leading to a noticeable reduction in the bulk density of the mixture. A similar reduction in density has been reported in studies involving other agricultural ashes such as rice husk ash and palm oil fuel ash, which are used as alternative fillers in asphalt mixtures.

3.5. X-ray diffraction (XRD) analysis

X-ray diffraction (XRD) was conducted to determine the mineralogical phases present in the Sugarcane Bagasse Ash (SBA) and granite aggregates (both coarse and fine). The XRD pattern of SBA displays a broad hump in the range of 20–30° (2θ), indicating a predominantly amorphous structure typical of amorphous silica (SiO_2). This amorphous nature is crucial for supporting the pozzolanic reactivity of SBA, making it a suitable mineral filler for asphalt applications. The minor crystalline peaks observed were attributed primarily to quartz and calcite, suggesting the presence of residual mineral phases owing to incomplete combustion or the original composition of the biomass, as shown in Fig. 9.

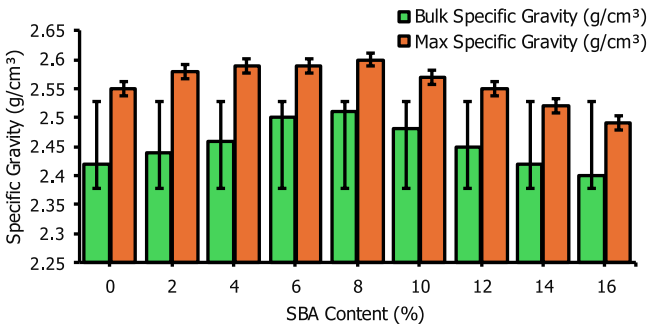

Fig. 8. A graph showing effect of sugarcane bagasse ash (SBA) on bulk specific gravity and maximum specific gravity.

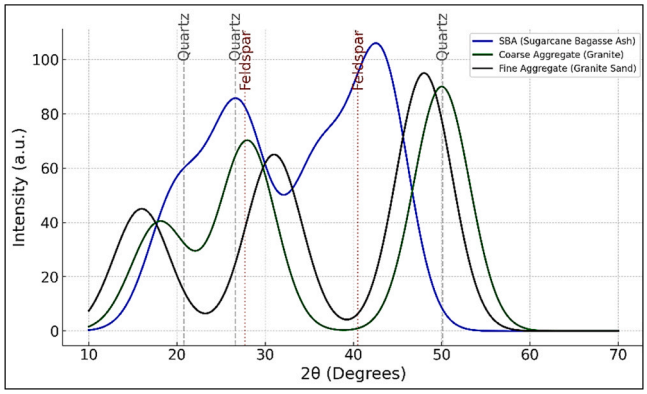

Fig. 9. X-ray diffraction (XRD) pattern of SBA, coarse and fine aggregate.

In contrast, the XRD patterns of the coarse and fine aggregates show sharp and well-defined peaks, indicative of a high degree of crystallinity. The dominant peaks corresponded to quartz (SiO_2) and feldspar ($KAlSi_3O_8$ – $NaAlSi_3O_8$), which are the principal mineral phases in granite. The presence of these crystalline structures confirms the suitability of the aggregates for use in hot mix asphalt (HMA) because they contribute to the mechanical strength, angularity, and durability of the final asphalt composite.

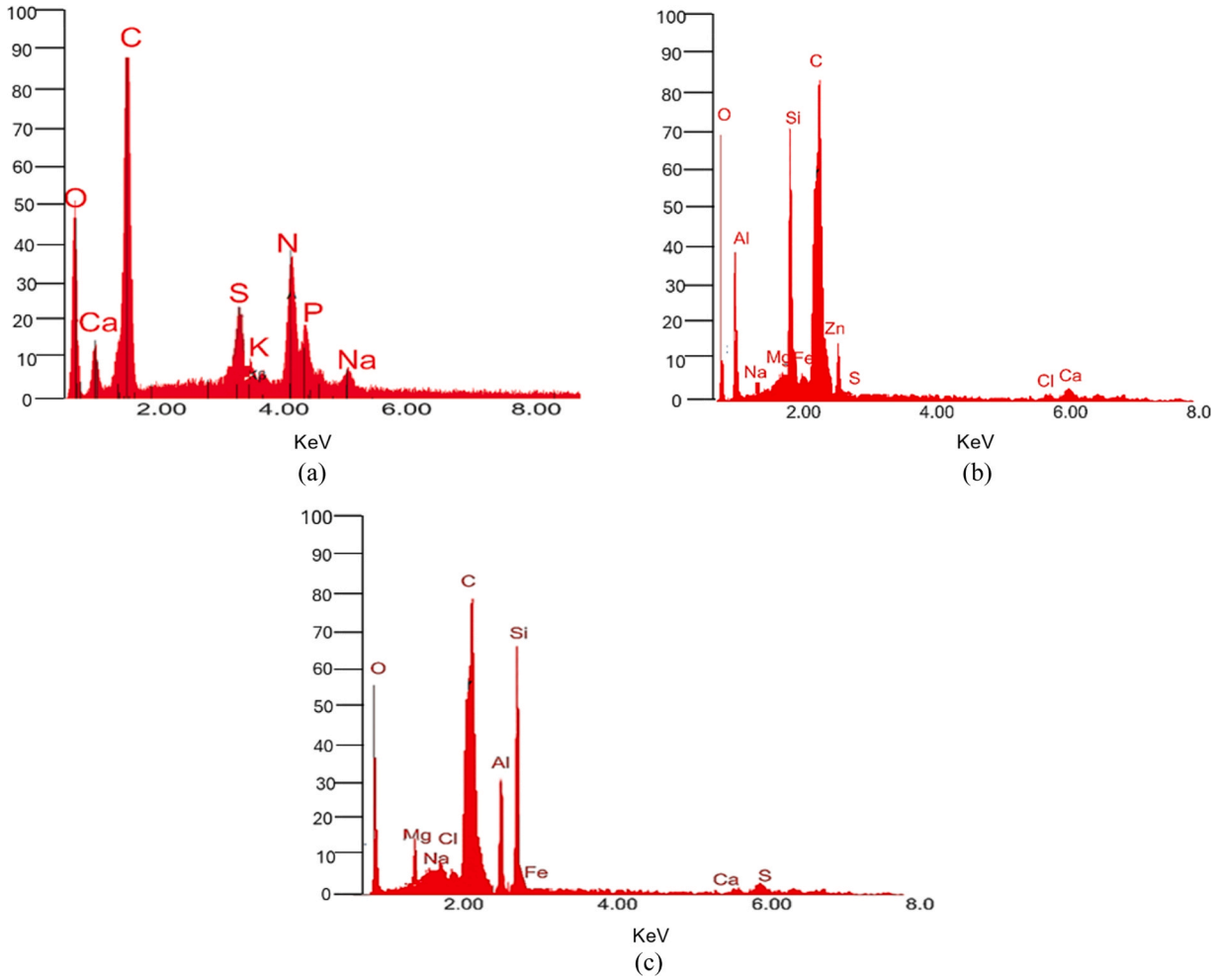

Fig. 10. Energy dispersive (EDS) spectroscopy; (a) bitumen; (b) asphalt; (c) SBA.

3.6. Energy dispersive X-ray (EDS) spectroscopy

Fig. 10. shows the energy-dispersive X-ray (EDS) spectra of (a) bitumen, (b) asphalt, and (c) Sugarcane Bagasse Ash (SBA), providing insight into the elemental composition of each material and their potential interactions in the composite formulations.

The EDX spectrum of bitumen (Fig. 9a) reveals a dominant carbon (C) peak with minor contributions from oxygen (O). This is consistent with the hydrocarbon-rich nature of bitumen, which is primarily composed of high-molecular-weight organic compounds. The negligible presence of inorganic elements confirms that the bitumen has a limited mineral content. In contrast, the asphalt sample (Fig. 9b) exhibits a more diverse elemental profile. In addition to carbon and oxygen, notable peaks were observed for silicon (Si), calcium (Ca), aluminum (Al), and iron (Fe). These elements originate from mineral aggregates and fillers incorporated into the asphalt mixture. The presence of these minerals is crucial for the mechanical strength and durability of asphalt pavements, which suggests that their inorganic content significantly affects the structural integrity of the composite. The SBA sample (Fig. 9c) exhibited high concentrations of silicon (Si), potassium (K), calcium (Ca), and oxygen (O), indicating silica-rich biomass ash. The elevated silica content suggests pozzolanic potential, making SBA a promising supplementary material for bitumen- and asphalt-based systems. Its composition is characteristic of agricultural waste ash and supports its reuse as a sustainable construction material. The progression from bitumen to SBA highlights the increasing presence of inorganic constituents, particularly silicon and calcium oxide. This transition has significant implications for material performance. Incorporating SBA into bituminous binders or asphalt mixtures can enhance stiffness, reduce the temperature susceptibility, and improve the resistance to oxidative aging. Therefore, EDX analysis supports the viability of SBA as an additive or partial replacement in asphalt formulations, contributing not only to improved performance but also to environmental sustainability through the valorization of agricultural waste.

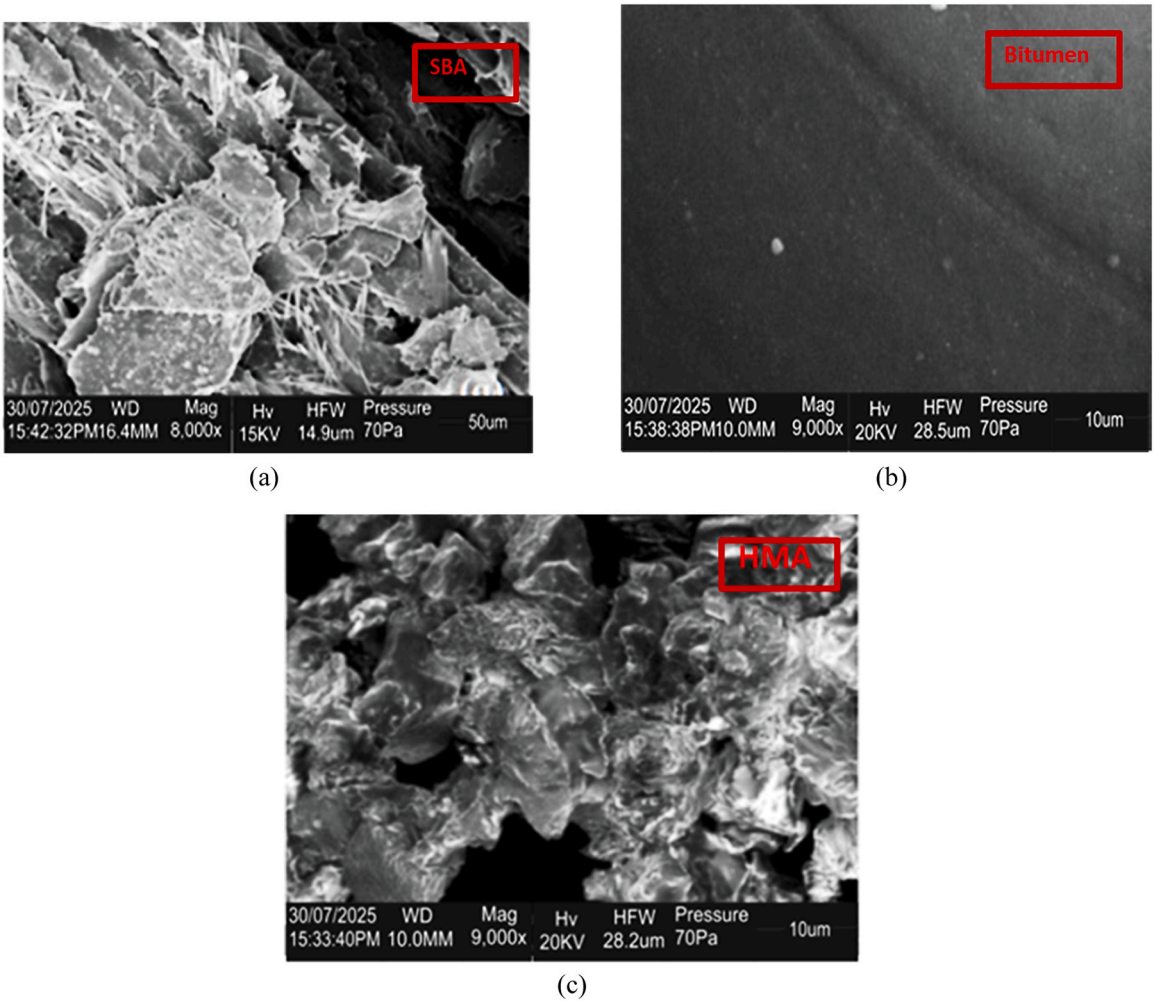

Fig. 11. Scanning electron microscopy (SEM) images of: (a) sugarcane bagasse ash (SBA) (scale bar = 50 μm, magnification = Mag 8000 ×); (b) SBA-modified bitumen (scale bar = 10 μm, magnification = Mag 9000 ×); and (c) unmodified asphalt (HMA) (scale bar = 10 μm, magnification = Mag 9000 ×).

3.7. Scanning electron microscopy (SEM) analysis

Scanning Electron Microscopy (SEM) was conducted to investigate the microstructural features of Sugarcane Bagasse Ash (SBA), unmodified bitumen, and SBA-modified bitumen. The SEM images are presented in Fig. 11, illustrating the (a) morphology of SBA, (b) microstructure of SBA-modified bitumen, and (c) surface texture of the unmodified bitumen. This comparatively uniform morphology reflects a lower internal structure, which may contribute to inferior performance under mechanical and thermal stresses. SEM analysis confirmed that the incorporation of SBA altered the microstructure of bitumen, indicating improved physical interaction, which may lead to enhanced performance properties such as stiffness, rutting resistance, and durability.

3.8. Preliminary life cycle and environmental assessment (LCA)

Although the primary focus of this study was to evaluate the mechanical, volumetric, and microstructural performance of SBA-modified asphalt mixtures, preliminary life-cycle screening was conducted to quantify the environmental implications of replacing a portion of the conventional mineral filler with Sugarcane Bagasse Ash (SBA). The aim of this assessment is not to provide a full pavement LCA but rather to estimate the order-of-magnitude carbon and resource savings associated with the optimal SBA incorporation identified experimentally (6–10 %, with a peak at 8 %).

3.8.1. Goal, scope, and functional unit

The LCA followed a cradle-to-gate system boundary (modules A1–A3), covering only the production of materials up to their delivery at the asphalt plant. The functional unit (FU) is 1 ton of Hot-Mix Asphalt (HMA) produced according to the mix design in Table 5. The scenarios were compared as follows:

- Reference mix (0 % SBA): 1-ton of HMA containing 150 kg of conventional quarry-derived mineral filler.
- SBA mix (8 % SBA): 1-ton of HMA containing 138 kg mineral filler and 12 kg SBA (8 % of filler by mass).

All other mixture components (aggregate gradation, 5.1 % binder content, heating energy, compaction, and plant operations) remained unchanged and therefore cancelled out at this screening stage.

3.8.2. System boundary and modelling assumptions

The assessment includes:

- Extraction, crushing, and milling of quarry-derived mineral filler.
- SBA processing (controlled combustion at 650 °C, grinding, sieving to < 75 μm).
- Short-haul Road transport of filler and SBA to the asphalt plant.

The following modelling assumptions were adopted based on commonly reported values in LCA databases:

- Cradle-to-gate emission factor for ground limestone/mineral filler: 0.039 kg CO_2e per kg of milled filler.
- SBA is treated as an agricultural residue from sugar processing; therefore, upstream cultivation burdens are not allocated to ash. Only incremental processing is performed.
- Grinding and sieving SBA to filler fineness requires approximately 25 kWh per tonne of SBA, equivalent to 0.018 kg CO_2e per kg SBA when applying an electricity emission factor of 0.7 kg CO_2e/kWh (typical for fossil-dominated grids in Sub-Saharan Africa).
- Transport emissions are very small compared to material production and are included within the literature ranges, but not itemized here. These assumptions represent a conservative but realistic approximation of the material-level impacts.

3.8.3. Life-cycle inventory and GHG estimation

Reference mix (0 % SBA): $CO_2e_{ref} = 150\ \text{kg} \times 0.039\ \text{kg}\ CO_2e/\text{kg} \approx 5.9\ \text{kg}\ CO_2e$ per tonne of HMA

SBA-modified mix (8 % SBA):

- Mineral filler: $138\ \text{kg} \times 0.039 = 5.42\ \text{kg}\ CO_2e$
- SBA processing: $12\ \text{kg} \times 0.018 = 0.22\ \text{kg}\ CO_2e$

Total:$CO_2\ e_{SBA\ mix} \approx 5.64\ \text{kg}\ CO_2e$ per tonne of HMA

Net GHG reduction $\Delta CO_2e = 5.90 - 5.64 = 0.26\ \text{kg}\ CO_2e$ per tonne of HMA

Thus, at the filler level, the 8 % SBA substitution achieves approximately:

- 4–8 % reduction in filler-related embodied carbon
- ≈ 0.5–1.0 % reduction in total HMA cradle-to-gate emissions (typical HMA: 40–70 kg CO_2e/t).

Although the total carbon reduction per ton is modest, reflecting the small mass share of the filler in HMA, the environmental benefit is systematic and scalable.

3.8.4. Landfill diversion and resource conservation

For every tonne of HMA produced with 8 % SBA:$m_{SBA} = 0.08 \times 150\ \text{kg} = 12\ \text{kg SBA/t HMA}$

Scaling this to a typical 2-lane, 40 mm wearing course:

Volume per kilometre:$7.3\ \text{m} \times 0.04\ \text{m} \times 1000\ \text{m}$

Using a compacted mix density of 2.45 t/m^3:$\approx$ 715t HMA per km

SBA incorporated:$715 \times 0.012 \approx 8.6$ t SBA diverted per km

GHG reduction per km:$0.26\ \text{kg CO}_2\text{e/t} \times 715\text{t} \approx 190\ \text{kg CO}_2\text{e}$ saved per km

Therefore, each kilometer of surface roadway constructed with the optimal 8 % SBA content valorizes 8–9 tons of waste bagasse ash, reduces quarry filler demand by the same amount, and achieves a measurable but modest reduction in embodied carbon.

3.8.5. Interpretation

Although the absolute carbon savings per ton are limited owing to the small mass fraction of fillers in HMA, the results highlight three important sustainability benefits.

- Circular material use: SBA transforms abundant agricultural residue into a valuable engineering material for road infrastructure.
- Resource conservation: Even a small percentage of substitutions reduces the dependence on quarry-derived fillers and the associated environmental burdens.
- Scalability: Given that road construction consumes millions of tons of HMA annually, even marginal CO_2 reductions (0.5–1 % per ton) and waste diversion of 8–9 t/km become highly significant at network scale.

These findings reinforce the role of SBA-modified HMA as a low-cost, low-carbon, resource-efficient pavement material suitable for sugarcane-producing regions, such as Nigeria and Sub-Saharan Africa.

4. Numerical analysis

4.1. Modal description

In this study, three-dimensional finite element modeling (FEM) was employed to simulate the mechanical behavior of Hot Mix Asphalt (HMA) with varying proportions of Sugarcane Bagasse Ash (SBA) as a mineral filler. The primary objective was to replicate the indirect tensile loading conditions defined by ASTM D6931 [64] and investigate the influence of SBA on the stress distribution, strain localization, and potential failure mechanisms. This modeling framework provides a deeper understanding of how SBA content affects the cracking resistance and structural integrity of asphalt mixtures.

4.2. Modeling software and approach

The simulation was conducted using Abaqus/CAE 2021, which is a widely recognized platform for advanced nonlinear and contact mechanics simulations. A 3D cylindrical geometry representing the standard Indirect Tensile Strength (ITS) test specimen (100 mm diameter $\times$ 63.5 mm height) was developed. The FEM simulations adopted a linear-elastic, homogeneous, and isotropic material law to enable a first-order comparison across SBA levels and to maintain the parameter space consistent with the experimental ITS inputs. However, asphalt exhibits pronounced temperature- and rate-dependent viscoelasticity, and a nonlinear response under higher strains. Consequently, the present model is best viewed as an initial approximation that reproduces stress distributions and peak tensile

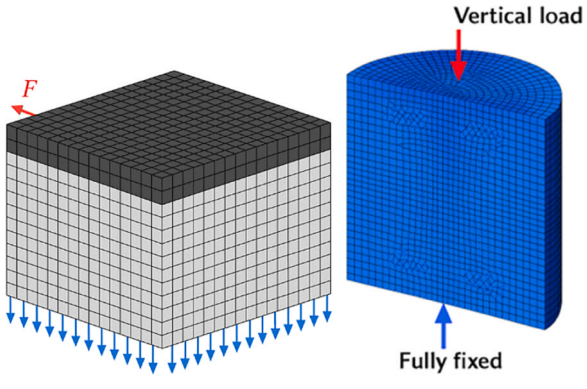

Fig. 12. 3D FEM mesh and boundary condition of the ITS specimen.

stresses in the quasilinear regime. Future work should employ thermo-viscoelastic or viscoelasto-plastic constitutive laws (e.g., generalized Maxwell/Prony series for binder–mastic or incremental plasticity for mixture nonlinearity), incorporate temperature/strain-rate coupling, and simulate cyclic loading and moisture conditioning to capture rutting, fatigue, and time-dependent damage more faithfully.

Modeling Assumptions and Conditions:

- Material Behavior: Linear elastic, homogeneous, and isotropic.
- Element Type: Eight-node 3D reduced integration brick elements (C3D8R) were used for discretization.
- Mesh Strategy: A fine mesh was applied near the load application zones to capture high-stress gradients, with a coarser mesh elsewhere to reduce the computation time.
- Boundary Conditions: The bottom surface of each specimen is fixed. A compressive load was applied along the vertical axis via semi-cylindrical rigid plates to induce an indirect tensile stress, as shown in Fig. 12.
- Symmetry: One-quarter model symmetry was utilized to minimize the computational demand without compromising accuracy.

4.3. Material properties

The material properties were assigned based on a combination of laboratory testing and relevant literature. Table 8 summarizes the key input parameters for the control and SBA-modified asphalt mixtures. The modulus of elasticity was adjusted for each SBA percentage, based on the experimental ITS results and regression correlations.

4.4. Simulation results and discussion

The developed 3D finite element model was used to examine the stress response of SBA-modified HMA specimens under indirect tensile loading and to identify the most critical tensile stress locations associated with crack initiation (Fig. 13). For all mixtures, the simulation reproduced the classical ITS stress state: maximum principal tensile stresses developed along the horizontal diameter and peaked at the specimen center, consistent with the theoretical splitting plane and the observed diametral cracking mode during laboratory testing.

4.4.1. Principal stress distribution and crack initiation zones

The principal stress contours show a concentrated tensile zone at the center of the specimen under diametral compression. This region represents the most likely crack initiation point, and the stress field extends along the horizontal diameter, supporting the experimentally observed failure pattern. The stress distribution was symmetric and stable, confirming that the boundary conditions and loading configuration realistically represent the ITS setup.

4.4.2. Effect of SBA content on stress localization

The simulations showed that SBA content influences both the magnitude and distribution of tensile stresses:

- Moderate SBA contents (6–8 %) produced a more uniform stress distribution across the central zone and reduced stress gradients near the loading line. This indicates improved internal load transfer and cohesion, which aligns with the experimentally observed increase in ITS within the same replacement range.
- Higher SBA contents (> 10 %) resulted in increased stress localization and higher peak tensile stresses at the specimen center. This behavior is consistent with a more brittle response and reduced tensile resistance, supporting the experimentally observed decline in ITS at higher replacement levels. The likely reason is that excessive SBA, owing to its porous and low-density nature, reduces packing efficiency and increases binder demand, which can weaken the mastic and reduce structural continuity.

The FEM results reinforce the experimentally identified optimal SBA window (6–10 %), by showing the transition from improved stress redistribution (beneficial) to localized tensile concentration (detrimental) as SBA content increases.

4.4.3. Mesh refinement and numerical stability

To ensure that the predicted peak tensile stresses were not dependent on discretization, a mesh refinement strategy was adopted. The mesh was locally refined at the load contact zones and the central tensile region, where steep stress gradients occur, while a coarser mesh was maintained elsewhere to reduce computational cost. A convergence check was performed by progressively refining the mesh until changes in the predicted peak tensile stress became negligible (variation within an acceptable tolerance). This confirms that the

Table 8
Modal material properties.

Property	Control Mix	SBA-Modified Mix
Elastic Modulus, E (MPa)	3500	2800–4200 (SBA-dependent)
Poisson's Ratio, ν	0.35	0.30–0.38
Density, ρ (kg/m^3)	2350	Measured per mix design

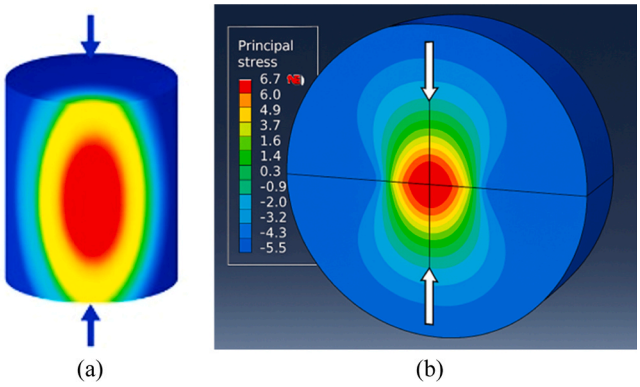

Fig. 13. Principal stress distribution Under various Loading condition (a).Indirect tensile stress (ITS) Loading (b) Diametral Loading.

reported stress contours and peak stresses reflect the material response rather than numerical artifacts.

4.4.4. Model scope and interpretation

It should be emphasized that the FEM framework adopts a linear-elastic, homogeneous, isotropic representation of asphalt mixtures. While asphalt behavior is inherently viscoelastic and temperature dependent, the chosen model is appropriate for capturing first-order stress patterns and comparative differences across SBA contents under quasi-static loading. Therefore, the numerical results are interpreted as mechanistic support for experimental trends rather than a full representation of time-dependent damage or fatigue behavior.

4.5. Model validation

The validity of the developed finite element model was evaluated by comparing the numerically predicted Indirect Tensile Strength (ITS) values with the corresponding experimental results obtained from laboratory testing as shown in Fig. 14. The validation focused on assessing the model's ability to reproduce the tensile response and cracking behavior of SBA-modified hot-mix asphalt mixtures under indirect tensile loading. Quantitative validation was performed using the coefficient of determination (R^2) and the root mean square error (RMSE) between the experimental and FEM-predicted ITS values. The computed values of $R^2 = 0.897$ and RMSE $= 0.024$ MPa indicate a strong correlation and low prediction error, demonstrating that the FEM successfully captures the dominant trends in tensile strength variation with SBA content in Fig. 15.

In addition to these statistical indicators, relative error bounds were evaluated to further assess prediction reliability. As summarized in Table 9, the FEM-predicted ITS values deviated from the experimental measurements by less than $\pm$ 10 % across all SBA replacement levels, with most deviations remaining below 3 %. These error bounds fall within acceptable limits for a simplified linear-elastic representation of heterogeneous asphalt mixtures and provide an additional measure of confidence in the numerical predictions.

Furthermore, the FEM-predicted principal tensile stress contours accurately reproduced the experimentally observed crack initiation zones, which consistently developed along the horizontal diameter at the specimen center. This agreement confirms that the numerical model not only predicts peak tensile strength values with reasonable accuracy but also represents the underlying stress concentration mechanisms governing diametral splitting failure in the ITS test.

Overall, the validation results confirm that the proposed FEM framework provides a reliable first-order approximation of the tensile behavior of SBA-modified HMA under quasi-static loading conditions. While the model does not explicitly account for viscoelasticity, damage evolution, or temperature-dependent effects, it is adequate for comparative analysis across SBA contents and for supporting the experimental findings. Future work will focus on incorporating viscoelastic constitutive models and cyclic loading conditions to further enhance predictive capability.

5. Conclusion

This study investigated the effect of Sugarcane Bagasse Ash (SBA) as a partial mineral filler replacement in hot-mix asphalt (HMA) through an integrated experimental and numerical approach. Based on the results, the following key conclusions are drawn:

- Optimal performance range: SBA can be effectively incorporated as a filler substitute in HMA within an optimal replacement range of 6–10 % by filler weight, with peak performance at approximately 8 % SBA. Within this range, the mixtures exhibited improved Marshall stability, stiffness, bulk density, and indirect tensile strength while maintaining air voids and volumetric parameters within standard design limits. SBA contents above 10 % led to reduced mechanical performance due to over-filling and reduced packing efficiency.

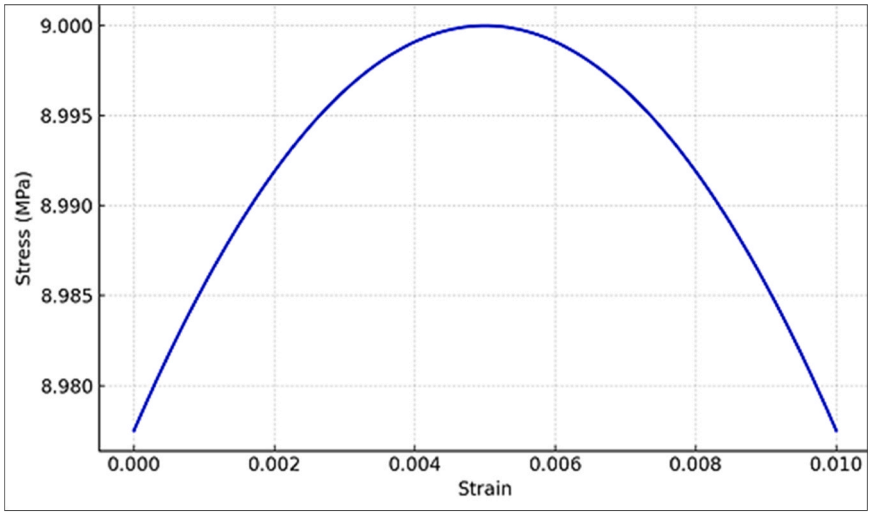

(a)

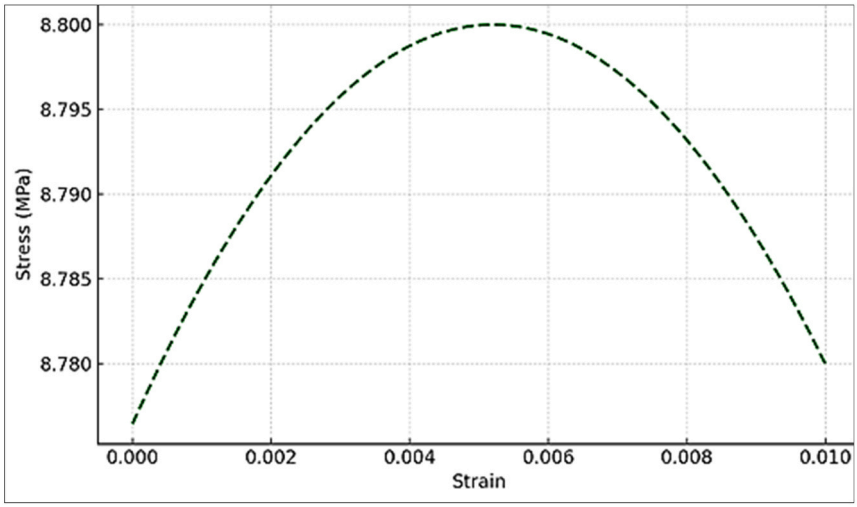

(b)

Fig. 14. Validation of experimental and FEM predicted stress-strain behavior of SBA-modified HMA (a). Experimental analysis; (b) FEM-predicted (numerical).

- Mechanistic validation: Microstructural analyses confirmed that SBA is predominantly composed of amorphous silica with a porous morphology, which enhances filler–binder interaction and mixture densification at moderate replacement levels. The three-dimensional finite element model successfully reproduced the experimentally observed tensile stress distribution and crack initiation behavior, with prediction errors generally below 10 %, providing mechanistic support for the laboratory findings.
- Sustainability and practical relevance: As an abundant agricultural residue, SBA offers a sustainable and cost-effective alternative to quarry-derived mineral fillers. Its use contributes to waste valorization, reduced natural resource consumption, and modest reductions in embodied carbon. The findings demonstrate that SBA-modified HMA is a technically viable and environmentally beneficial option, particularly for sugarcane-producing regions such as sub-Saharan Africa.

Overall, the study provides a clear performance-based framework for incorporating SBA into asphalt mixtures and supports its practical application in sustainable pavement engineering.

6. Recommendations for future Work

The numerical model adopted a linear–elastic homogeneous material description and did not explicitly simulate viscoelasticity, moisture damage, or cyclic loading. Therefore, future research should consider the following.

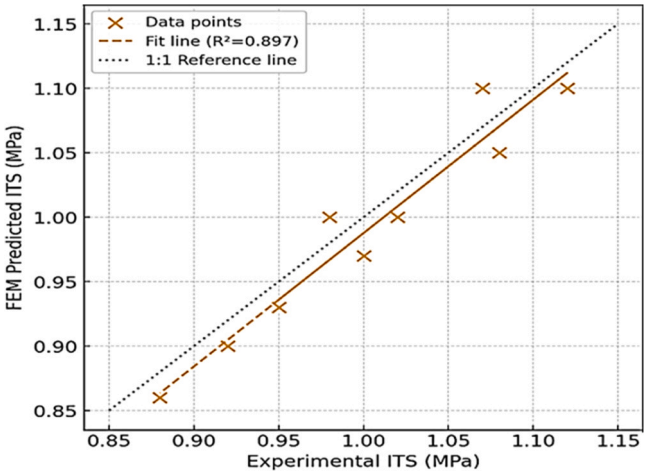

Fig. 15. Correlation between experimental and FEM-predicted indirect tensile strength (ITS) values for sugarcane bagasse ash (SBA)-modified hot-mix asphalt.

Table 9
Experimental vs. FEM indirect tensile strength (ITS) across SBA contents with absolute and relative errors.

SBA (%)	Experimental ITS (MPa)	FEM ITS (MPa)	Absolute Error (MPa)	Relative Error (%)
0	0.95	0.93	0.02	2.1
2	0.98	1.00	0.02	2.0
4	1.02	1.00	0.02	2.0
6	1.08	1.05	0.03	2.8
8	1.12	1.10	0.02	1.8
10	1.07	1.10	0.03	2.8
12	1.00	0.97	0.03	3.0
14	0.92	0.90	0.02	2.2
16	0.88	0.86	0.02	2.3

- Implement thermo-viscoelastic or viscoelasto-plastic constitutive models and cyclic loading to capture rutting and fatigue more realistically.
- Extend testing to moisture susceptibility (TSR), aging, and long-term durability under local traffic and climate conditions.
- Conduct a full life-cycle assessment (LCA) and cost–benefit analyses that include plant energy use, transport, and end-of-life scenarios.
- Validation of the laboratory and FEM findings through field trials and performance monitoring of SBA-modified pavements.

Within the limitations of the present work, it can be concluded that sugarcane bagasse ash, when used at controlled levels (6–10 %) as a partial filler replacement, enhances the sustainable performance of hot-mix asphalt and provides a technically and environmentally sound pathway for valorizing agricultural waste in pavement engineering.

CRediT authorship contribution statement

Adeyemi Oluwaseun Adeboje: Validation, Methodology, Conceptualization. **Udeme Udo Imoh:** Writing – original draft, Visualization, Validation, Software, Methodology, Data curation, Conceptualization. **Majid Movahedi Rad:** Writing – review & editing, Supervision. **Rauf Hassan:** Visualization, Validation, Data curation. **Ebunlomo Ruth Adekola:** Writing – original draft.

Funding

This study did not receive external funding.

Declaration of Competing Interest

The authors declare that they have no known competing financial interests or personal relationships that could have appeared to influence the work reported in this paper.

Acknowledgements

The authors acknowledge the support of those who contributed directly and indirectly to the success of this study.

Data availability

Data will be made available on request.

References

[1] W.S. Alaloul, K.M. Alzubi, A.B. Malkawi, M. Al Salaheen, M.A. Musarat, Productivity monitoring in building construction projects: a systematic review, Eng. Constr. Archit. Manag. 29 (2022) 2760–2785, https://doi.org/10.1108/ECAM-03-2021-0211.
[2] N. García-Troncoso, S. Hidalgo-Astudillo, K. Tello-Ayala, N. Vanegas-Alman, D.V. Bompa, Preparation and performance of sugarcane bagasse ash pavement repair mortars, Case Stud. Constr. Mater. 19 (2023) e02563, https://doi.org/10.1016/j.cscm.2023.e02563.
[3] A. Tripathy, P.K. Acharya, Characterization of bagasse ash and its sustainable use in concrete as a supplementary binder – a review, Constr. Build. Mater. 322 (2022) 126391, https://doi.org/10.1016/j.conbuildmat.2022.126391.
[4] A.A.A. Apata, A.C.U.U. Imoh, Pavement design of Ilaro- Papa Alanto Highway, Ogun State, Nigeria, Int. J. Innov. Sci. Res. Technol. 7 (2022) 11–22.
[5] I.N. Usanga, U.U. Imoh, E.M. Imitini, J. Etuke, Evaluation of mechanical properties of asphalt-concrete using Baghouse dust as filler material, Evaluation 6 (2021).
[6] A.H. Albayati, A review of rutting in asphalt concrete pavement, Open Eng. 13 (2023), https://doi.org/10.1515/eng-2022-0463.
[7] R. Joumblat, Z. Al Basiouni Al Masri, G. Al Khateeb, A. Elkordi, A.R. El Tallis, J. Absi, State-of-the-art review on permanent deformation characterization of asphalt concrete pavements, Sustainability 15 (2023) 1166, https://doi.org/10.3390/su15021166.
[8] H. Divandari, Predict of asphalt rutting potential based on IDT and validation with ANN, J. Appl. Eng. Sci. 9 (2019) 131–138, https://doi.org/10.2478/jaes-2019-0018.
[9] M. Chen, J. Lin, S. Wu, Potential of recycled fine aggregates powder as filler in asphalt mixture, Constr. Build. Mater. 25 (2011) 3909–3914, https://doi.org/10.1016/j.conbuildmat.2011.04.022.
[10] Z. Jwaida, Q.A. Al Quraishy, R.R.A. Almuhanna, A. Dulaimi, L.F.A. Bernardo, J.M. de A. Andrade, The use of waste fillers in asphalt mixtures: a comprehensive review, CivilEng 5 (2024) 801–826, https://doi.org/10.3390/civileng5040042.
[11] C. Dimulescu, A. Burlacu, Industrial waste materials as alternative fillers in asphalt mixtures, Sustainability 13 (2021) 8068, https://doi.org/10.3390/su13148068.
[12] A.C. Apata, U.U. Imoh, A Comparative Study of Strength Characteristics of Cold and Hot Asphalt Mixes Available for Road Maintenance in Lagos State, 2022. https://doi.org/10.5281/zenodo.6090934.
[13] U.U. Imoh, R. Nagy, M. Movahedi Rad, Micro-mechanical characterization of polymer-modified asphalt mixtures using discrete element modelling with soft-bond and linear contact bond models, Constr. Build. Mater. 501 (2025) 144325, https://doi.org/10.1016/j.conbuildmat.2025.144325.
[14] K. Zhang, J. Kevern, Review of porous asphalt pavements in cold regions: the state of practice and case study repository in design, construction, and maintenance, J. Infrastruct. Preserv. Resil. 2 (2021), https://doi.org/10.1186/s43065-021-00017-2.
[15] D. Jin, J. Wang, L. You, D. Ge, C. Liu, H. Liu, Z. You, Waste cathode-ray-tube glass powder modified asphalt materials: Preparation and characterization, J. Clean. Prod. 314 (2021) 127949, https://doi.org/10.1016/j.jclepro.2021.127949.
[16] F. Barraj, S. Mahfouz, H. Kassem, J. Khatib, D. Goulias, A. Elkordi, Investigation of using crushed glass waste as filler replacement in hot asphalt mixtures, Sustainability 15 (2023) 2241, https://doi.org/10.3390/su15032241.
[17] J. Wu, X. Ye, H. Cui, Recycled materials in construction: trends, status, and future of research, Sustainability 17 (2025) 2636, https://doi.org/10.3390/su17062636.
[18] D. Jin, T.K. Meyer, S. Chen, K. Ampadu Boateng, J.M. Pearce, Z. You, Evaluation of lab performance of stamp sand and acrylonitrile styrene acrylate waste composites without asphalt as road surface materials, Constr. Build. Mater. 338 (2022) 127569, https://doi.org/10.1016/j.conbuildmat.2022.127569.
[19] B.W. Colbert, Z. You, Properties of modified asphalt binders blended with electronic waste powders, J. Mater. Civ. Eng. 24 (2012) 1261–1267, https://doi.org/10.1061/(ASCE)MT.1943-5533.0000504.
[20] G.Z. Seitenova, R.M. Dyussova, D.A. Aspanbetov, A.Y. Jexembayeva, K. Korniejenko, L. Aruova, D.K. Sakanov, Eco-friendly bitumen composites with polymer and rubber waste for sustainable construction, Buildings 15 (2025) 2608, https://doi.org/10.3390/buildings15152608.
[21] D. Jin, L. Yin, L. Malburg, Z. You, Laboratory evaluation and field demonstration of cold in-place recycling asphalt mixture in Michigan low-volume road, Case Stud. Constr. Mater. 20 (2024) e02923, https://doi.org/10.1016/j.cscm.2024.e02923.
[22] D. Jin, K. Xin, L. Yin, S. Mohammadi, B. Cetin, Z. You, Performance of rubber modified asphalt mixture with tire-derived aggregate subgrade, Constr. Build. Mater. 449 (2024) 138261, https://doi.org/10.1016/j.conbuildmat.2024.138261.
[23] S. Barbhuiya, T. Qureshi, B.B. Das, Advancing sustainable pavements: a review of low-carbon construction materials and practices, Discov. Concr. Cem. 1 (2025) 19, https://doi.org/10.1007/s44416-025-00020-w.
[24] J.-S. Lee, S.-Y. Lee, Y.-S. Bae, T.H.M. Le, Development of pavement material using crumb rubber modifier and graphite nanoplatelet for pellet asphalt production, Polymers 15 (2023) 727, https://doi.org/10.3390/polym15030727.
[25] S. Lenart, S.R. Karumanchi, Deformation properties and performance evaluation of reused ballast with waste tire-derived aggregates, Transp. Geotech. 52 (2025) 101586, https://doi.org/10.1016/j.trgeo.2025.101586.
[26] D. Jin, S. Mohammadi, K. Xin, L. Yin, Z. You, Laboratory performance and field demonstration of asphalt overlay with recycled rubber and tire fabric fiber, Constr. Build. Mater. 438 (2024) 136941, https://doi.org/10.1016/j.conbuildmat.2024.136941.
[27] D. Ge, D. Jin, C. Liu, J. Gao, M. Yu, L. Malburg, Z. You, Laboratory performance and field case study of asphalt mixture with sasobit treated aramid fiber as modifier, Transp. Res. Rec.: J. Transp. Res. Board 2676 (2022) 811–824, https://doi.org/10.1177/03611981211047833.
[28] D. Jin, L. Yin, S. Nedrich, K.A. Boateng, Z. You, Resurface of rubber modified asphalt mixture with stress absorbing membrane interlayer: from laboratory to field application, Constr. Build. Mater. 441 (2024) 137452, https://doi.org/10.1016/j.conbuildmat.2024.137452.
[29] S. Chhetri, P. Deb, Finite element analysis of geogrid-incorporated flexible pavement with soft subgrade, Appl. Sci. 14 (2024) 5798, https://doi.org/10.3390/app14135798.
[30] M.A.S. Hadi, M.H. Al-Sherrawi, The influence of base layer thickness in flexible pavements, Eng. Technol. Appl. Sci. Res. 11 (2021) 7904–7909, https://doi.org/10.48084/etasr.4573.
[31] N. Mashaan, A. Chegenizadeh, H. Nikraz, Evaluating the rheological properties and ageing resistance of waste PET-modified bitumen binder, J. Kejuruter. 33 (2021) 679–689, https://doi.org/10.17576/jkukm-2021-33(3)-26.
[32] H. Osman, M.Z.I. Muhamad Rodzey, M.R. Mohd Hasan, T.L.X. Wong, M.F.H. Mohd Ghazali, Z. Zakaria, M. Jameel, Review of bonding behavior, mechanisms, and characterization approach in bituminous materials under different conditions, J. Traffic Transp. Eng. (Engl. Ed.) 11 (2024) 1291–1316, https://doi.org/10.1016/j.jtte.2024.06.002.
[33] G. Devecseri, Effect of heating on the physical properties of asphalt aggregates, Period. Polytech. Civ. Eng. 54 (2010) 53, https://doi.org/10.3311/pp.ci.2010-1.06.

[34] M.J. Vámos, J. Szendefy, Temperature effects on traffic load-induced accumulating strains in flexible pavement structures, Int. J. Pavement Res. Technol. (2024), https://doi.org/10.1007/s42947-024-00466-4.
[35] Z. Jwaida, A. Dulaimi, M.A.O. Mydin, Y.O. Özkılıç, R.P. Jaya, A. Ameen, The use of waste polymers in asphalt mixtures: bibliometric analysis and systematic review, J. Compos. Sci. 7 (2023) 415, https://doi.org/10.3390/jcs7100415.
[36] J. Pang, Y. Chen, L. Jing, H. Song, Z. Liu, Performance evaluation of warm-mix asphalt binders with an emphasis on rutting and intermediate-temperature cracking resistance, Materials 18 (2025) 1571, https://doi.org/10.3390/ma18071571.
[37] Z. Jwaida, A. Dulaimi, M.A.O. Mydin, Y.N. Kadhim, S. Al-Busaltan, The self-healing performance of asphalt binder and mixtures: a state-of-the-art review, Innov. Infrastruct. Solut. 9 (2024) 247, https://doi.org/10.1007/s41062-024-01547-w.
[38] Y. Liu, Z. Liu, Y. Zhu, H. Zhang, A review of sustainability in hot asphalt production: greenhouse gas emissions and energy consumption, Appl. Sci. 14 (2024) 10246, https://doi.org/10.3390/app142210246.
[39] A.O. Adeboje, O.A. Afinni, S.J. Adeniyi, T.C. Adelowo, S.O. Ademokoya, A.E. Adeniran, Influence of aluminium dross on the marshall properties of asphalt mixture, LAUTECH J. Civ. Environ. Stud. 14 (2025), https://doi.org/10.36108/laujoces/5202.41.0180.
[40] S.O. Olopade, A.O. Adeboje, A.O. Olutaiwo, A.A. Obisanya, Comparative evaluation of the engineering properties of asphaltic concrete from selected asphalt plants in southwestern Nigeria for road construction, Int. J. Sustain. Constr. Eng. Technol. 14 (2023), https://doi.org/10.30880/ijscet.2023.14.01.030.
[41] M. Paliukaitė, A. Vaitkus, A. Zofka, Evaluation of bitumen fractional composition depending on the crude oil type and production technology, in: Proceedings of the 9th International Conference "Environmental Engineering 2014," Vilnius Gediminas Technical University Press "Technika" 2014, Vilnius, Lithuania, 2014. https://doi.org/10.3846/enviro.2014.162.
[42] M. Kamran, M.T. Khan, D. Khan, M.R.M. Hasan, N. Khan, M. Ullah, Experimental evaluation of hot mix asphalt using coal bottom ash as partial filler replacement, Roads Bridges - Drog. i Mosty 22 (2023) 167–179, https://doi.org/10.7409/rabdim.023.008.
[43] N. Khan, F. Karim, Q.B.A.I. Latif Qureshi, S.A. Mufti, M.B.A. Rabbani, M.S. Khan, D. Khan, Effect of fine aggregates and mineral fillers on the permanent deformation of hot mix asphalt, Sustainability 15 (2023) 10646, https://doi.org/10.3390/su151310646.
[44] Z. Jwaida, Q.A. Al Quraishy, R.R.A. Almuhanna, A. Dulaimi, L.F.A. Bernardo, J.M. de A. Andrade, The use of waste fillers in asphalt mixtures: a comprehensive review, CivilEng 5 (2024) 801–826, https://doi.org/10.3390/civileng5040042.
[45] J. Styer, L. Tunstall, A. Landis, J. Grenfell, Innovations in pavement design and engineering: a 2023 sustainability review, Heliyon 10 (2024) e33602, https://doi.org/10.1016/j.heliyon.2024.e33602.
[46] D. Khan, R. Khan, M.T. Khan, M. Alam, T. Hassan, Performance of hot-mix asphalt using polymer-modified bitumen and marble dust as a filler, J. Traffic Transp. Eng. (Engl. Ed.) 10 (2023) 385–398, https://doi.org/10.1016/j.jtte.2022.12.002.
[47] U.U. Imoh, R. Nagy, M. Movahedi Rad, Micro-mechanical characterization of polymer-modified asphalt mixtures using discrete element modelling with soft-bond and linear contact bond models, Constr. Build. Mater. 501 (2025) 144325, https://doi.org/10.1016/j.conbuildmat.2025.144325.
[48] ASTM D4402/D4402M, Test Method for Viscosity Determination of Asphalt at Elevated Temperatures Using a Rotational Viscometer, ASTM International, 2023, https://doi.org/10.1520/D4402_D4402M-23.
[49] Y.O. Hetemoğlu, M.K. Çubuk, M. Gürü, Improvement in performance characteristics of bitumen and bituminous mixtures by means of polyvinyl acetate, Constr. Mater. 5 (2025) 9, https://doi.org/10.3390/constrmater5010009.
[50] S.T. Olalekan, A.A. Olatunde, S.K. Kolapo, J.M. Omolola, O.A. Olukemi, A. Ayanniyi Mufutau, O.O. Olaosebikan, A.A. Saka, Durability of bitumen binder reinforced with polymer additives: towards upgrading Nigerian local bitumen, Heliyon 10 (2024) e30825, https://doi.org/10.1016/j.heliyon.2024.e30825.
[51] ASTM C136/C136M, Test Method for Sieve Analysis of Fine and Coarse Aggregates, ASTM International, West Conshohocken, PA, 2025, https://doi.org/10.1520/C0136_C0136M-25.
[52] ASTM D70/D70M, Test Method for Density of Semi-Solid Asphalt Binder (Pycnometer Method), ASTM International, West Conshohocken, PA, 2021, https://doi.org/10.1520/D0070_D0070M-21.
[53] ASTM D4791, Test Method for Flat Particles, Elongated Particles, or Flat and Elongated Particles in Coarse Aggregate, ASTM International, West Conshohocken, PA, 2023, https://doi.org/10.1520/D4791-19R23.
[54] ASTM C131, Test Method for Resistance to Degradation of Small-Size Coarse Aggregate by Abrasion and Impact in the Los Angeles Machine, ASTM International, West Conshohocken, PA, 2020, https://doi.org/10.1520/C0131_C0131M-20.
[55] ASTM D5, Test Method for Penetration of Bituminous Materials, ASTM International, West Conshohocken, PA, 2020, https://doi.org/10.1520/D0005_D0005M-20.
[56] ASTM D6926, Practice for Preparation of Asphalt Mixture Specimens Using Marshall Apparatus, ASTM International, West Conshohocken, PA, 2020, https://doi.org/10.1520/D6926-20.
[57] ASTM D2042, Test Method for Solubility of Asphalt Materials in Trichloroethylene, ASTM International, West Conshohocken, PA, 2022, https://doi.org/10.1520/D2042-22.
[58] ASTM D36, Test Method for Softening Point of Bitumen (Ring-and-Ball Apparatus), ASTM International, West Conshohocken, PA, 2020, https://doi.org/10.1520/D0036_D0036M-14R20.
[59] ASTM D92, Test Method for Flash and Fire Points by Cleveland Open Cup Tester, ASTM International, West Conshohocken, PA, 2024, https://doi.org/10.1520/D0092-24.
[60] ASTM D6913, Test Methods for Particle-Size Distribution (Gradation) of Soils Using Sieve Analysis, ASTM International, West Conshohocken, PA, 2017, https://doi.org/10.1520/D6913_D6913M-17.
[61] ASTM C127, Test Method for Relative Density (Specific Gravity) and Absorption of Coarse Aggregate, ASTM International, West Conshohocken, PA, 2025 (⟨https://doi.org/10.1520/C0127-25⟩).
[62] ASTM C128, Test Method for Relative Density (Specific Gravity) and Absorption of Fine Aggregate, ASTM International, 2025, https://doi.org/10.1520/C0128-25.
[63] ASTM D946, Specification for Penetration-Graded Asphalt Binder for Use in Pavement Construction, ASTM International, West Conshohocken, PA, 2025, https://doi.org/10.1520/D0946_D0946M-25.
[64] ASTM D6931, Test Method for Indirect Tensile (IDT) Strength of Asphalt Mixtures, ASTM International, West Conshohocken, PA, 2024, https://doi.org/10.1520/D6931-24.